The Abdus Salam
International Centre for Theoretical Physics

United Nations
Educational, Scientific and
Cultural Organization

IAEA
International Atomic Energy Agency

2333-26

Workshop on Science Applications of GNSS in Developing Countries (11-27 April), followed by the: Seminar on Development and Use of the Ionospheric NeQuick Model (30 April-1 May)

11 April - 1 May, 2012

Sensing Space Weather with Distributed Observatories

VALLADARES Cesar

Institute for Scientific Research Boston College
St. Clement's Hall, 140 Commonwealth Avenue
CHESTNUT HILL MA 02467-3862
Massachusetts
U.S.A.

Sensing Space Weather with Distributed Observatories

Cesar E. Valladares

LISN
Low-Latitude Ionospheric Sensor Network

NSF

BOSTON COLLEGE
ISR
INSTITUTE FOR SCIENTIFIC RESEARCH

Low-latitude Ionospheric Sensor Network (LISN)

- The LISN network is a distributed observatory designed to provide nearly real-time observables (nowcast) to the Aeronomy community. LISN aims to develop a short term (60 minutes) predictive model of the ionosphere (forecast) based on real-time data-ingestion techniques.

- The main goal of LISN was to establish a permanent array of instruments to investigate the complex day-to-day variability and the extreme state of disturbance that occurs in the equatorial ionosphere in a regional context.

- LISN consists of: 46 GPS receivers, 5 magnetometers, and VIPIR ionosondes.

Outline

Science highlights of GPS receivers: Regional maps of TEC, regional maps of TEC depletions, study of TIDs.

VIPIR ionosondes science projects. E_s layer detections. Simultaneous measurements with the Jicamarca digisonde.

Science highlights based on magnetometer datasets. Longitudinal variability of ExB drifts and TEC. Measurements during disturbed and quiet magnetic conditions.

LISN: Toward forecasting ESF.

Locations of LISN GPS Receivers (46)

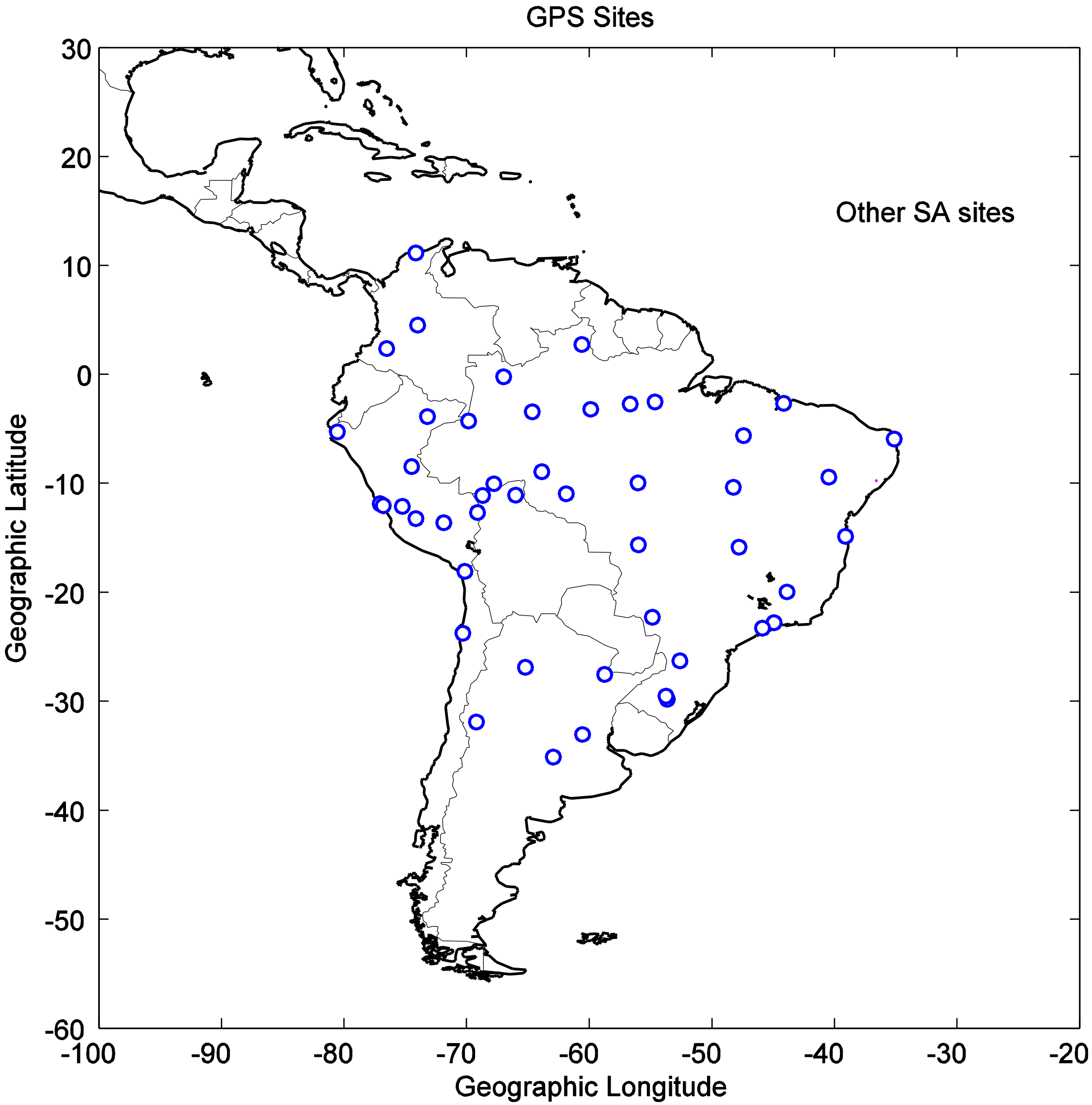

Locations of GPS Receivers over South America (~200)

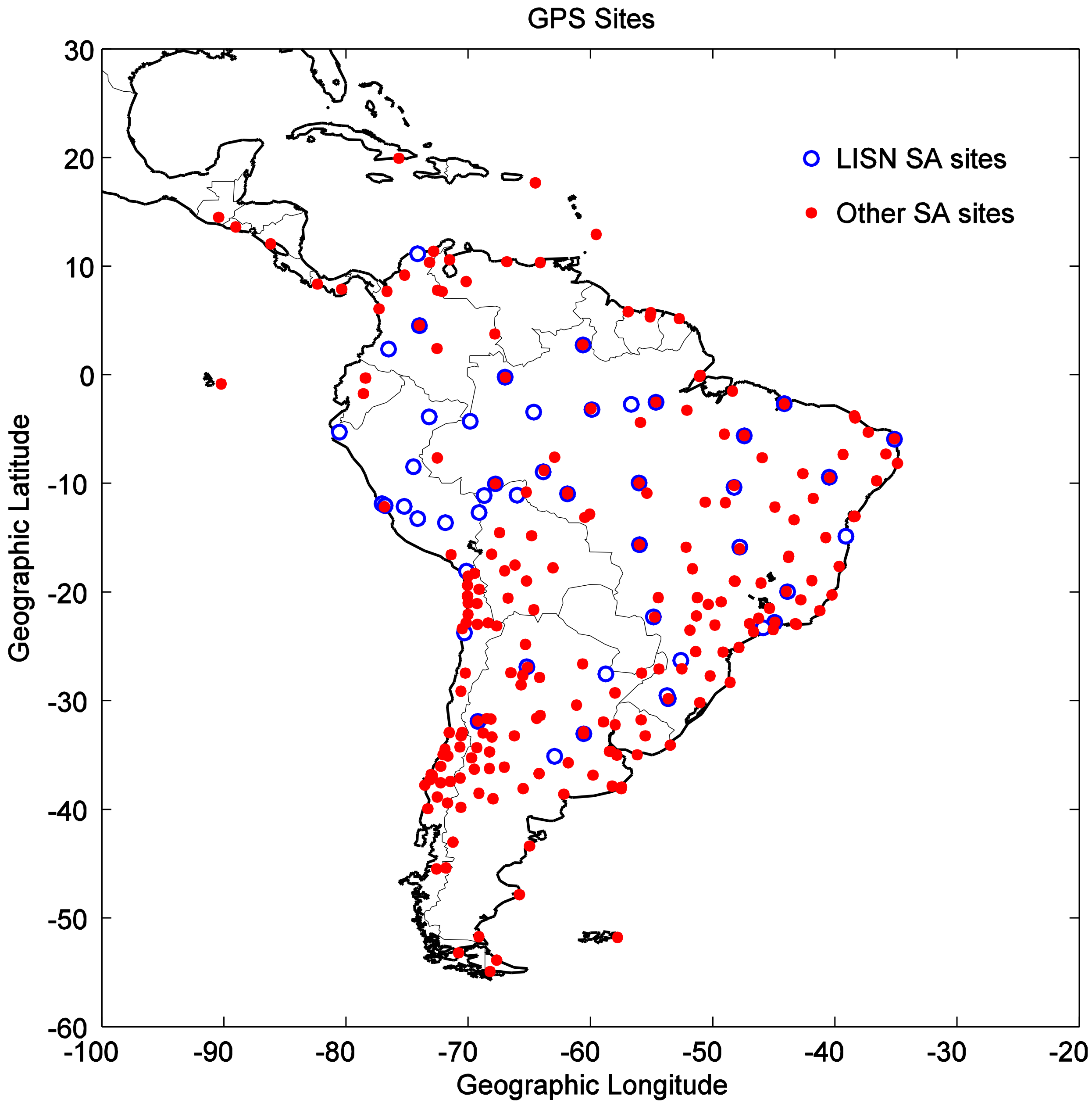

TEC observed on October 16, 2008

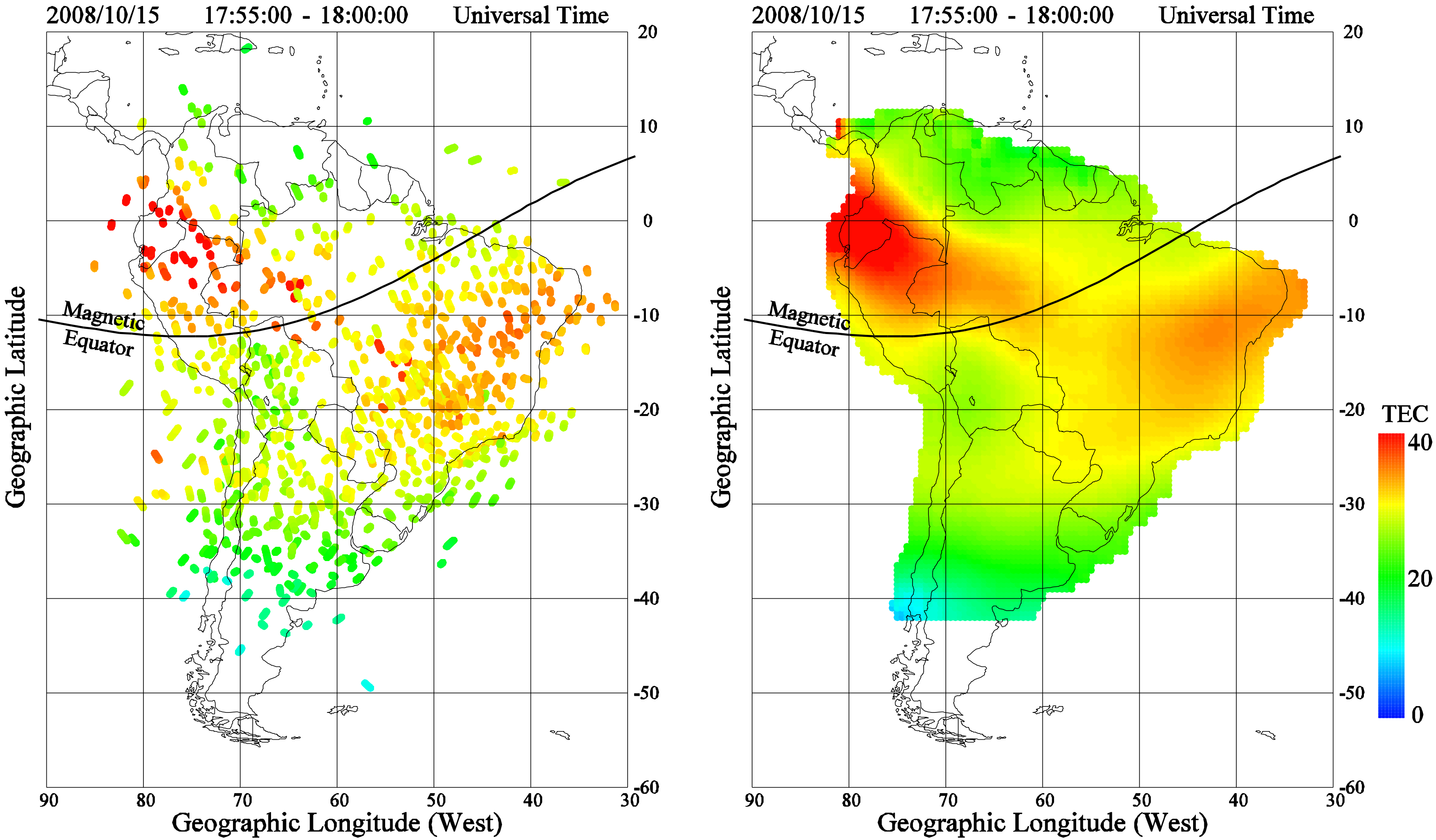

Characterize TEC variability in a regional Context: TEC values observed on 3 consecutive days (Oct 15-18, 2008) at same local time (2 PM at 60 W)

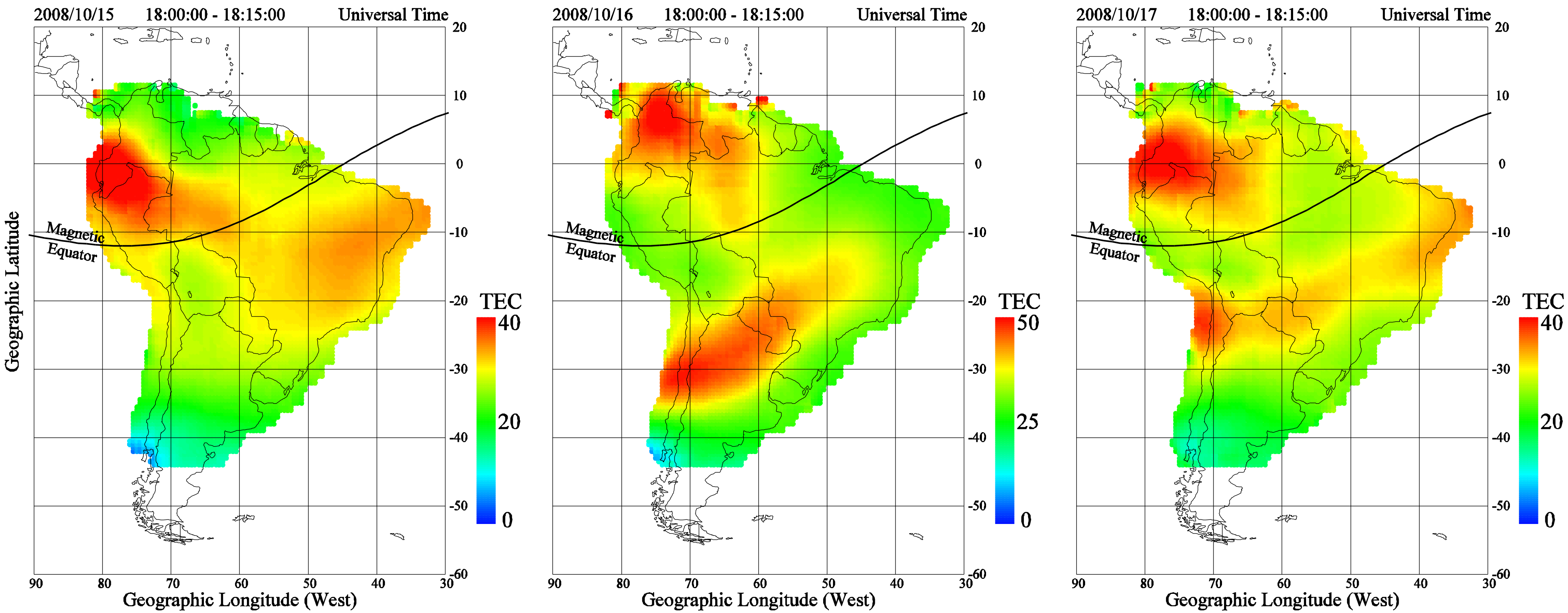

TEC depletions observed in November 07 and 08, 2008

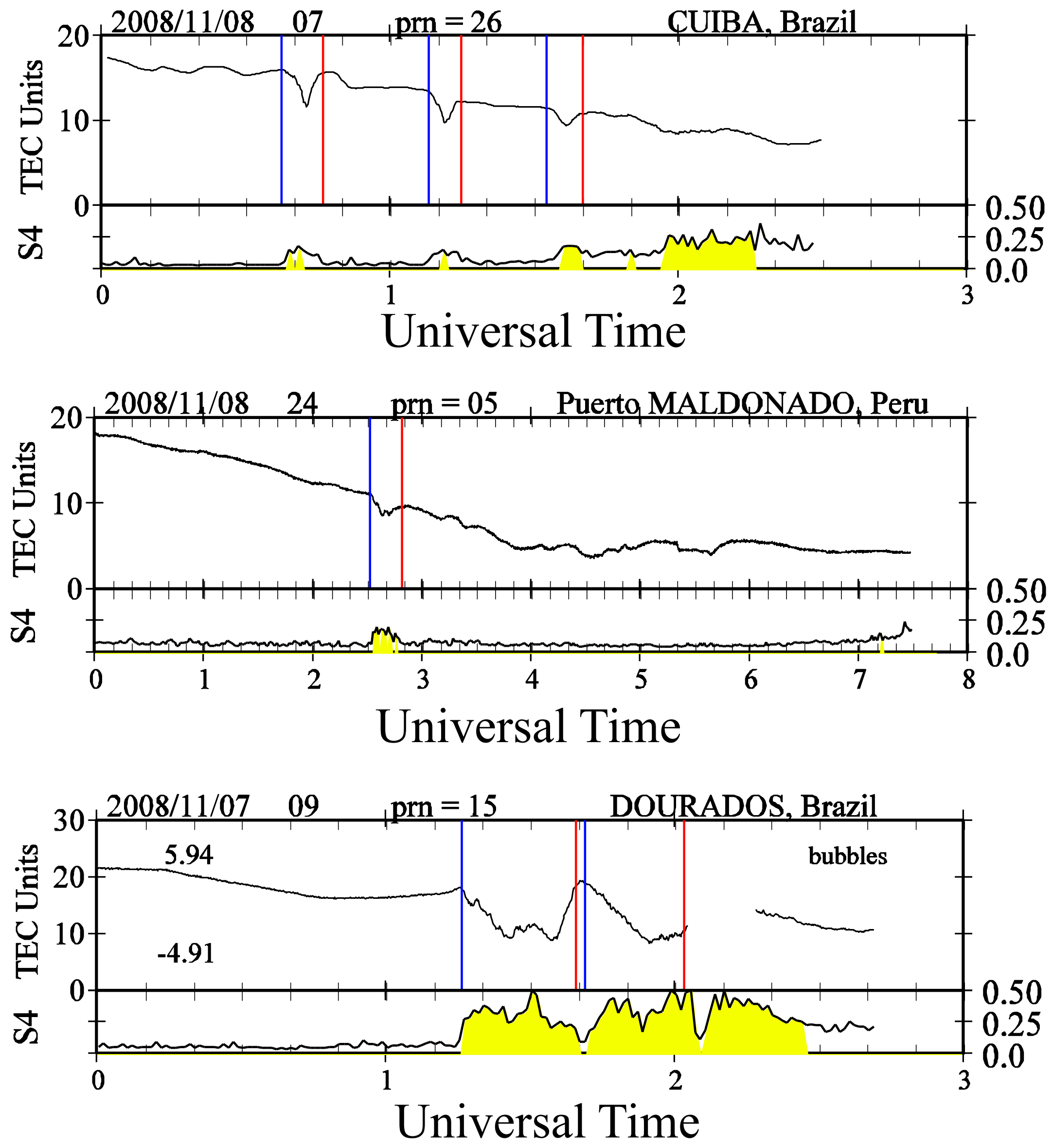

Seasonal Variability of TEC depletions that follow **Tsunoda's** 1985

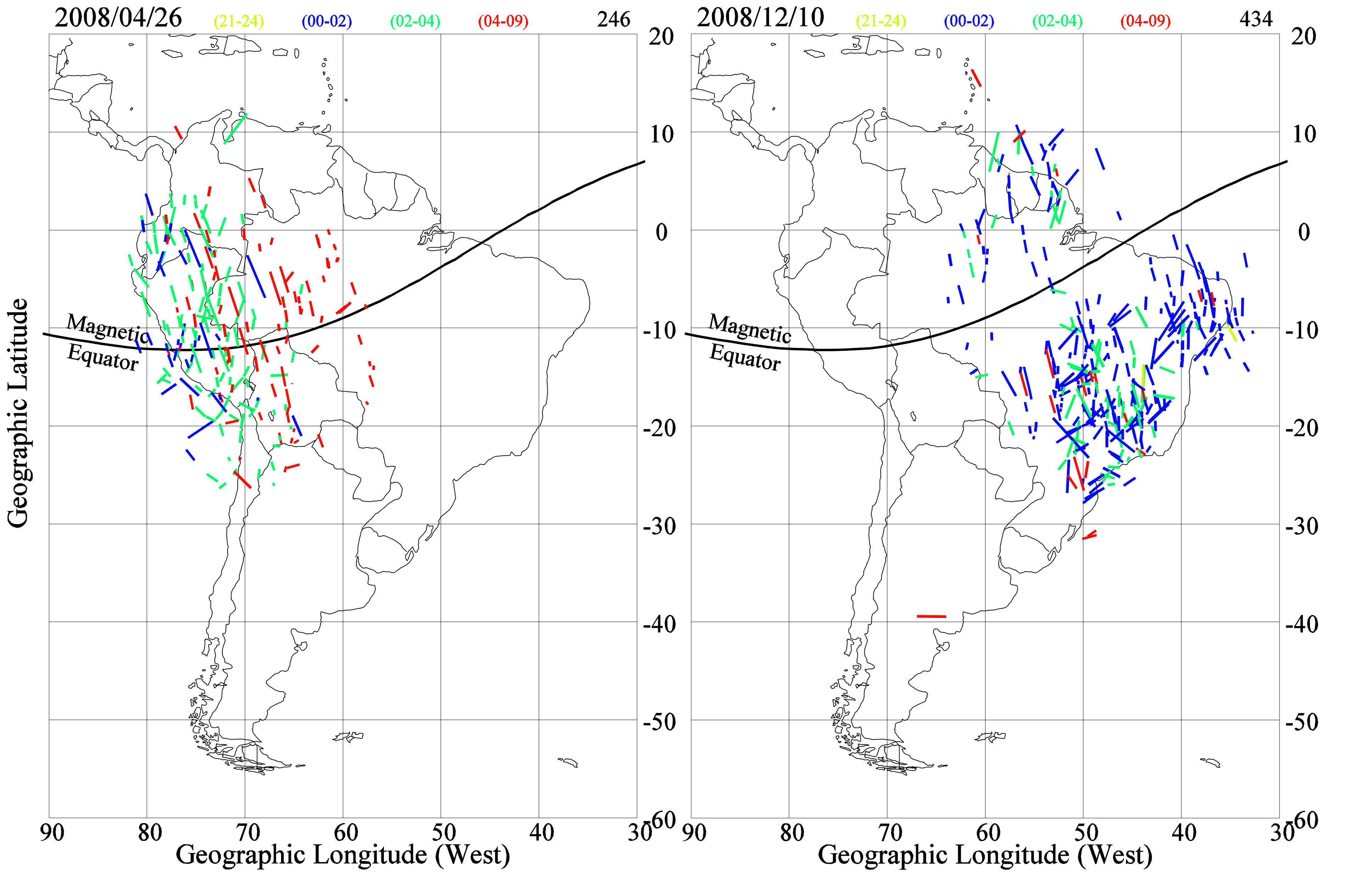

TEC depletions and TIDs in Two different sectors

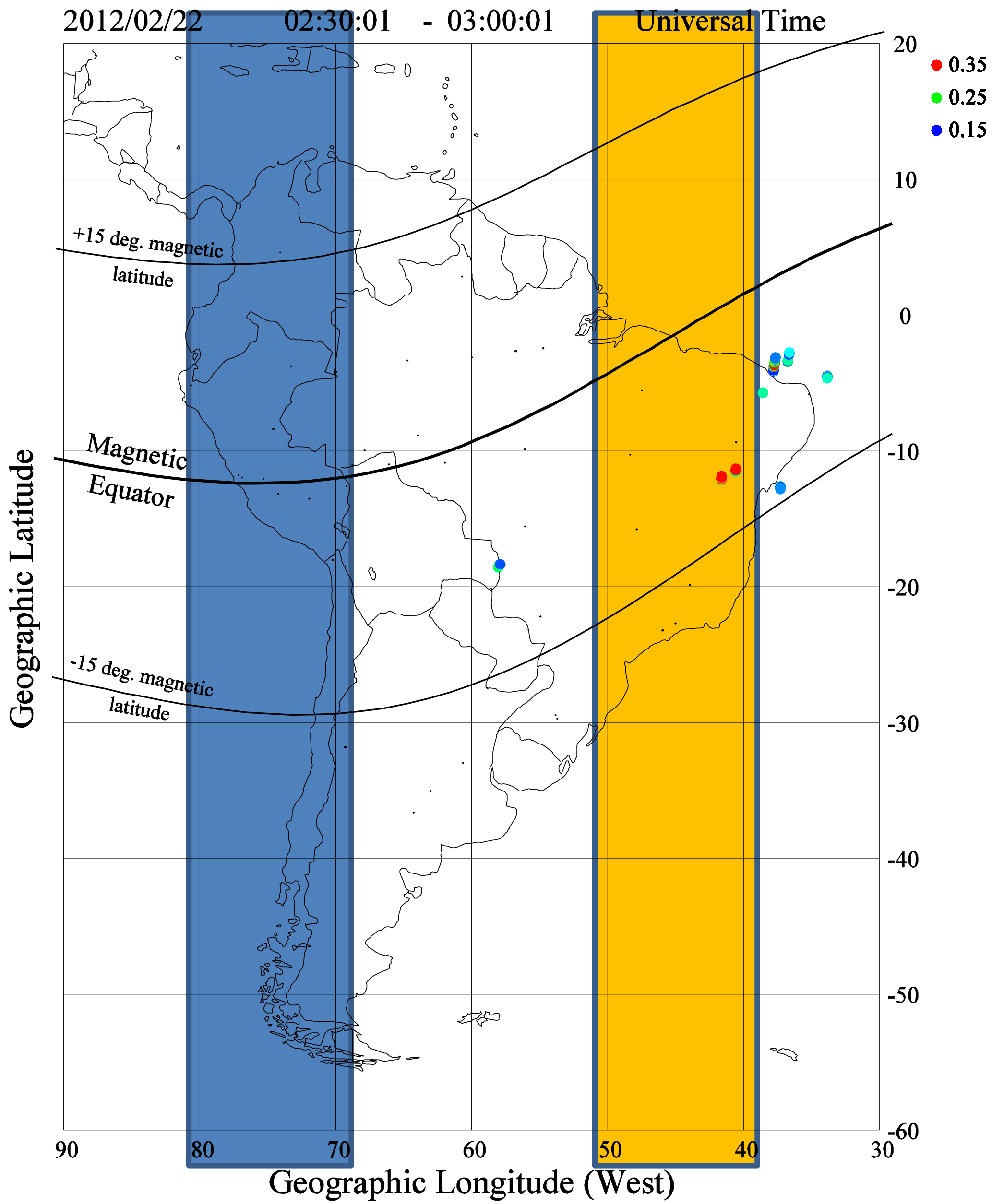

Number of TEC depletion detections as a function of Local time and day of Year

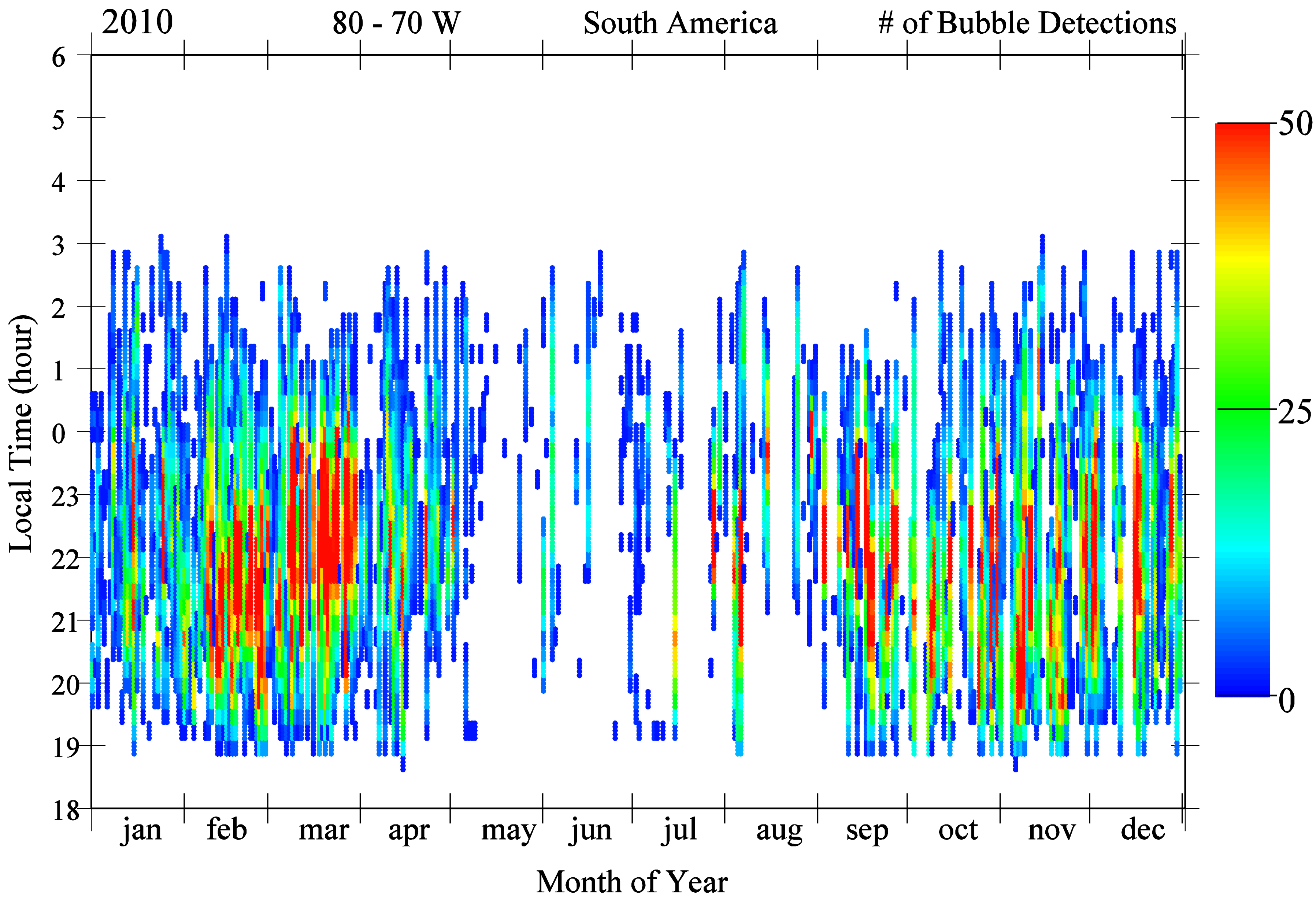

Number of TEC depletion detections as a function of Local time and day of Year

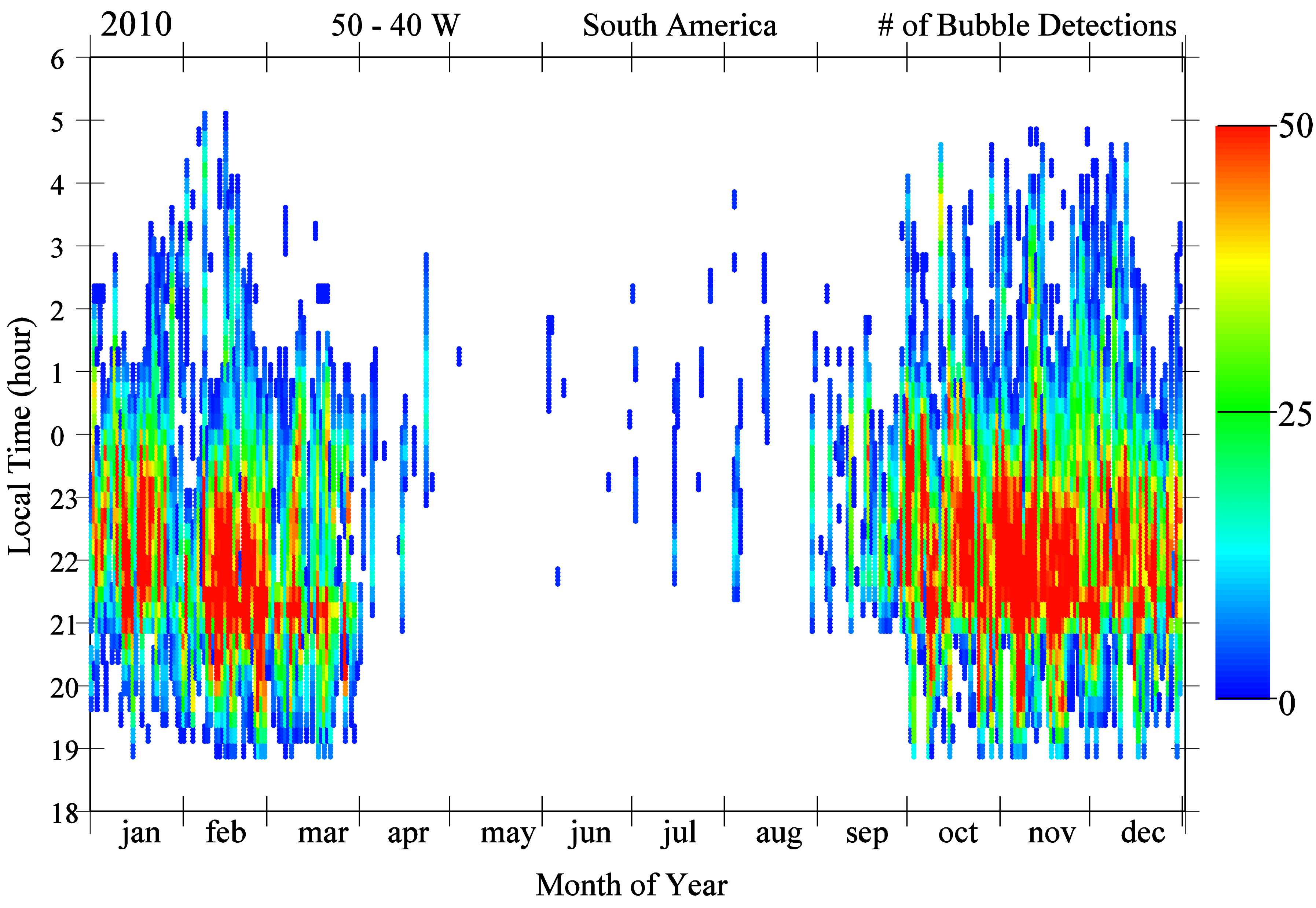

LISN GPS Network & 3 more Networks

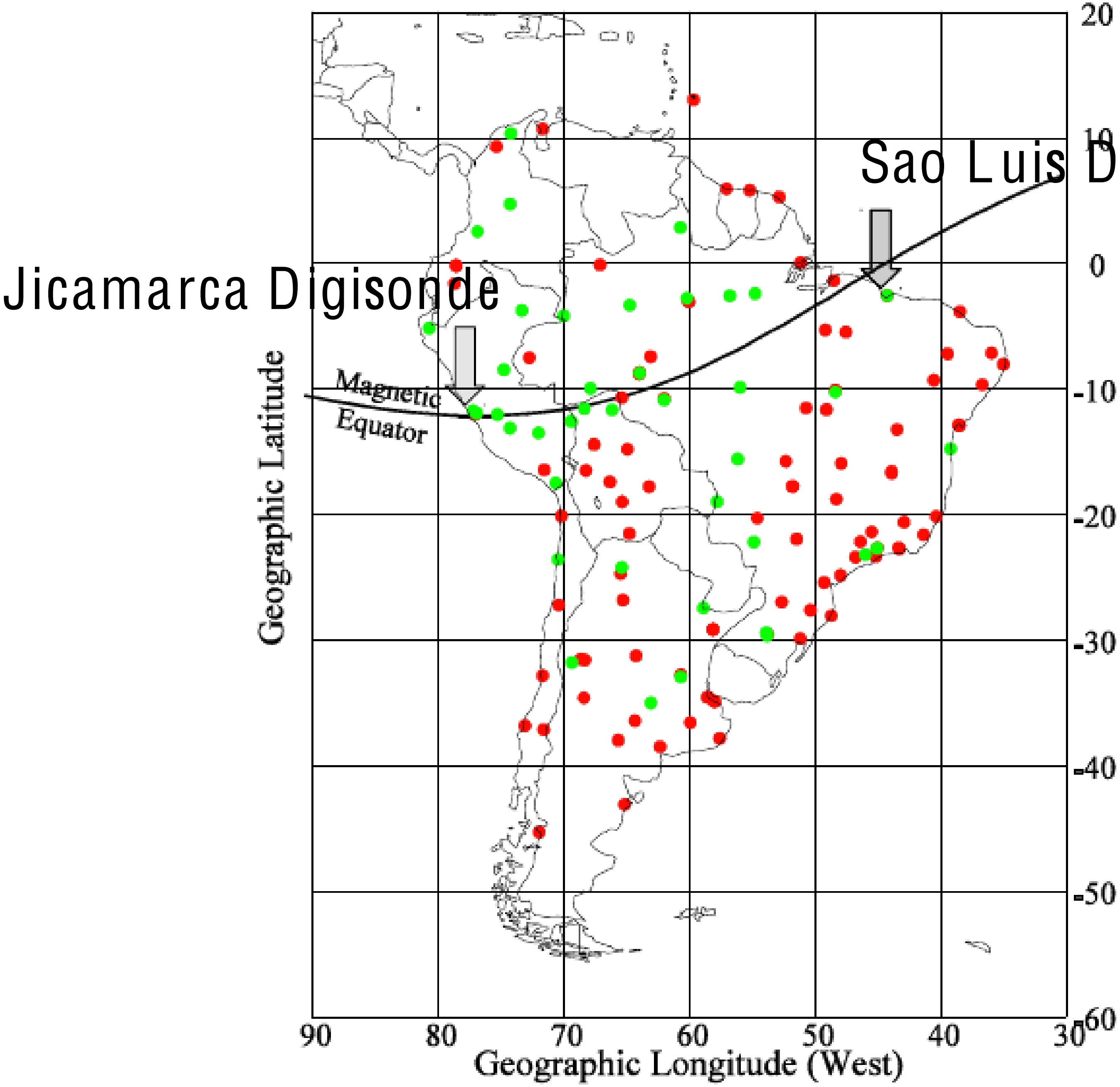

Preconditioning of the Ionosphere: Altitude of the F-layer (Farley et al., 1970). Magnitude of the Pre-reversal enhancement (Fejer et al., 1999) >20 m/s.

True heights and velocities for Jicamarca and Sao Luis for Dec 26, 2009 (LT)

Jicamarca

ROJ 360/2009

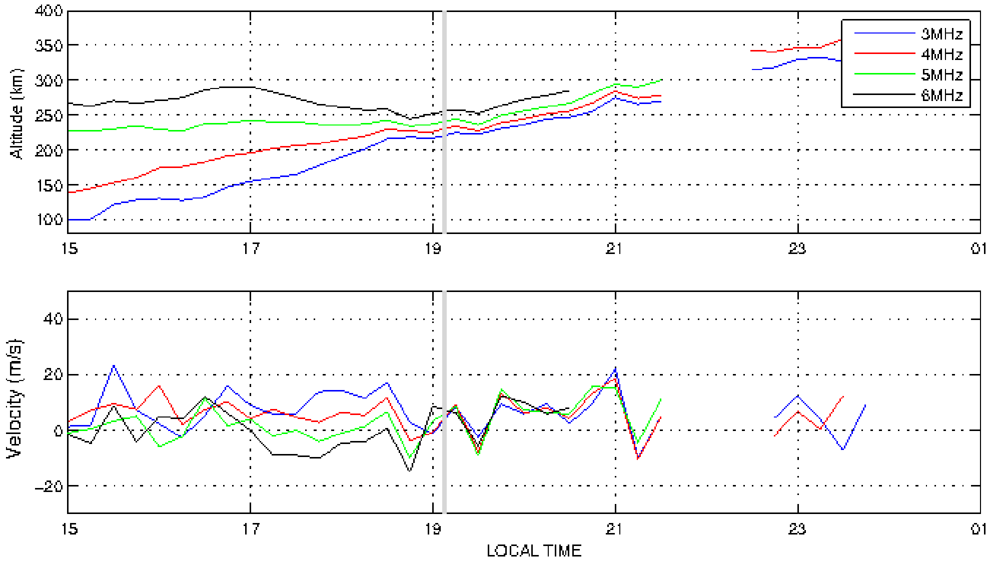

Sao Luis

SLZ 360/2009

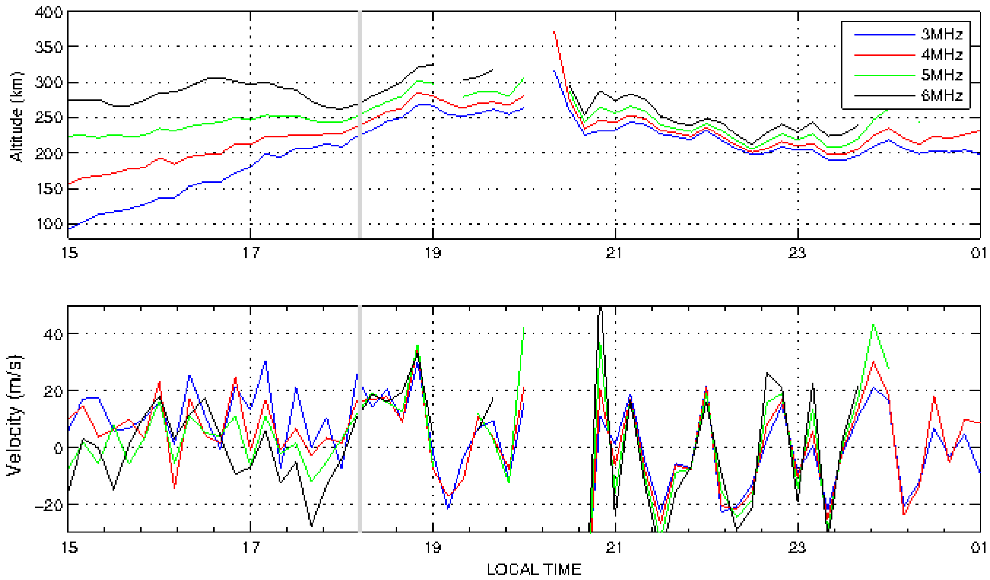

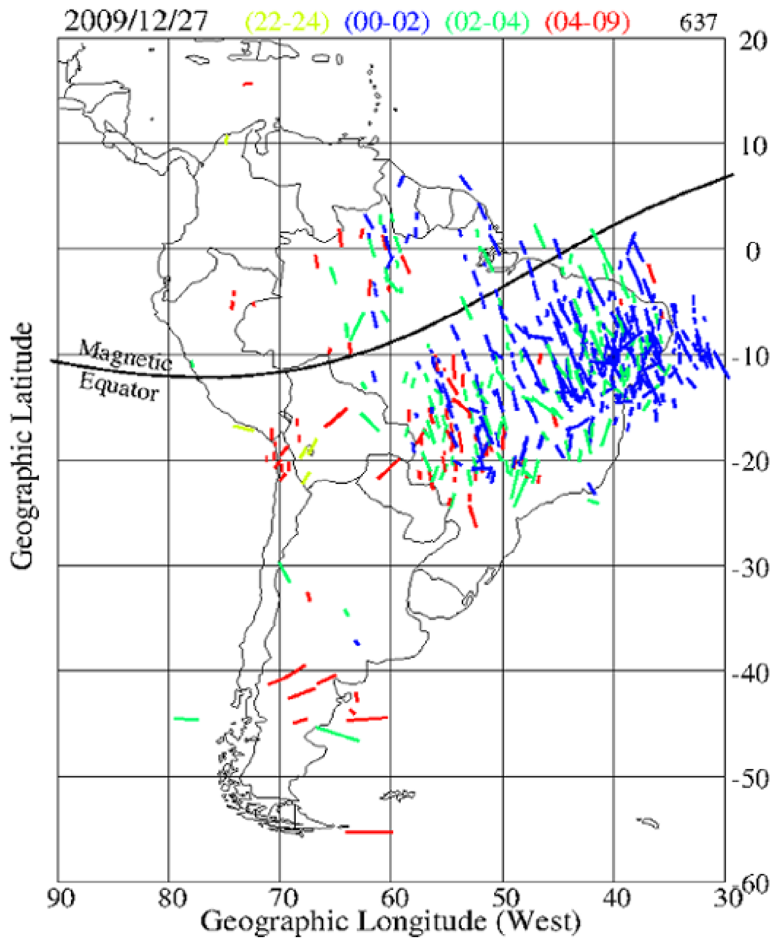

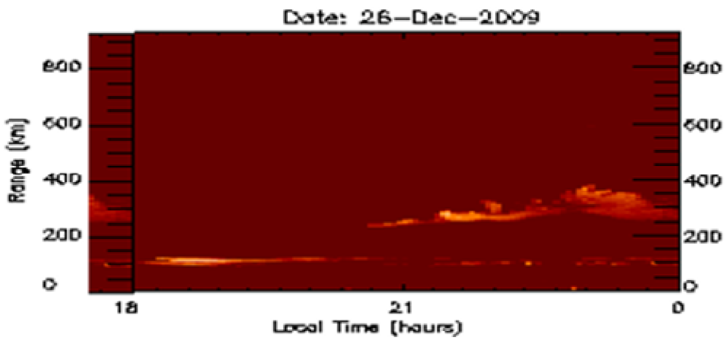

Identifying TIDs using TEC traces from Copiapo, Chile

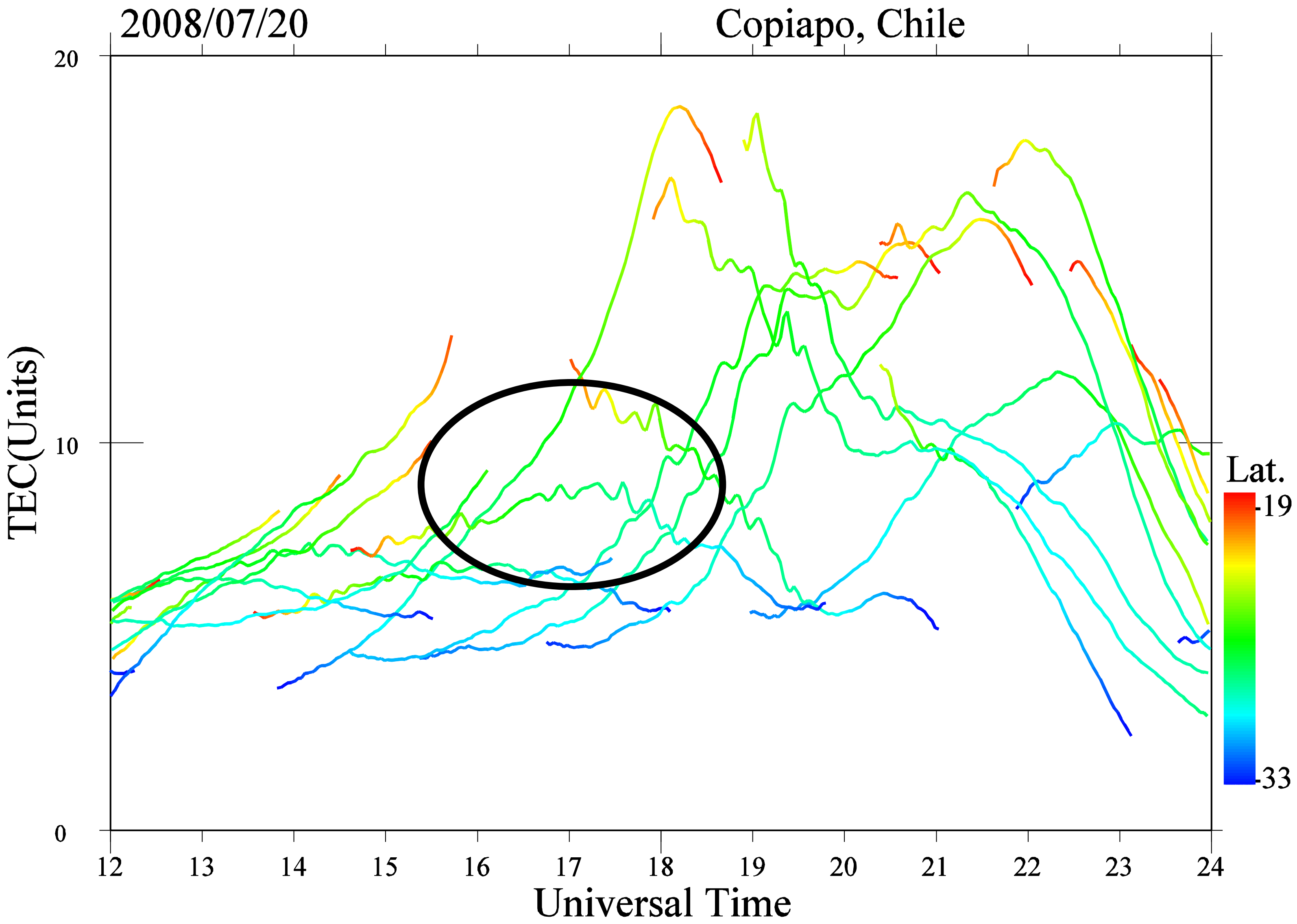

Location of 3 GPS receivers near Huancayo

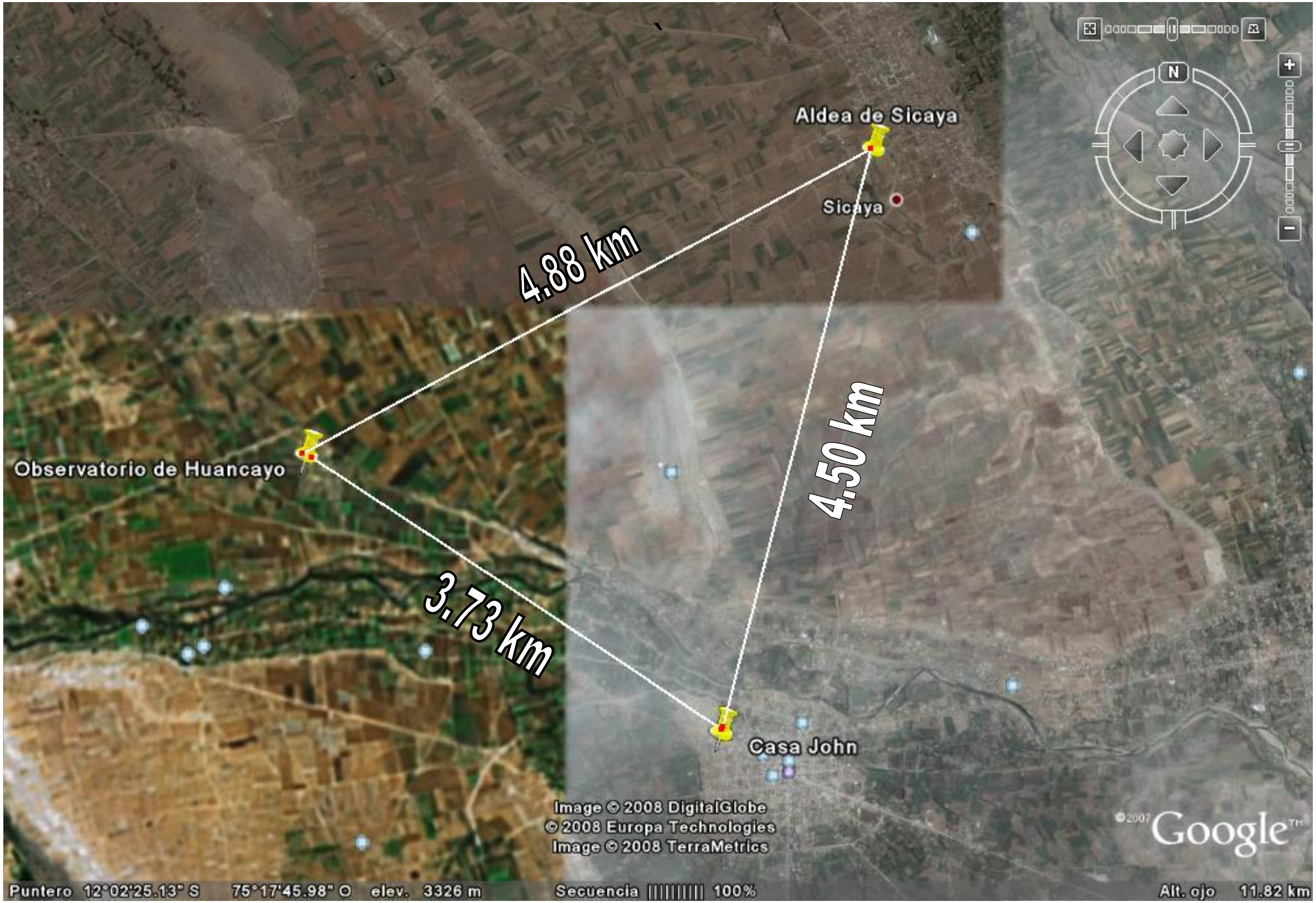

TEC values measured at Huancayo on July 20, 2008

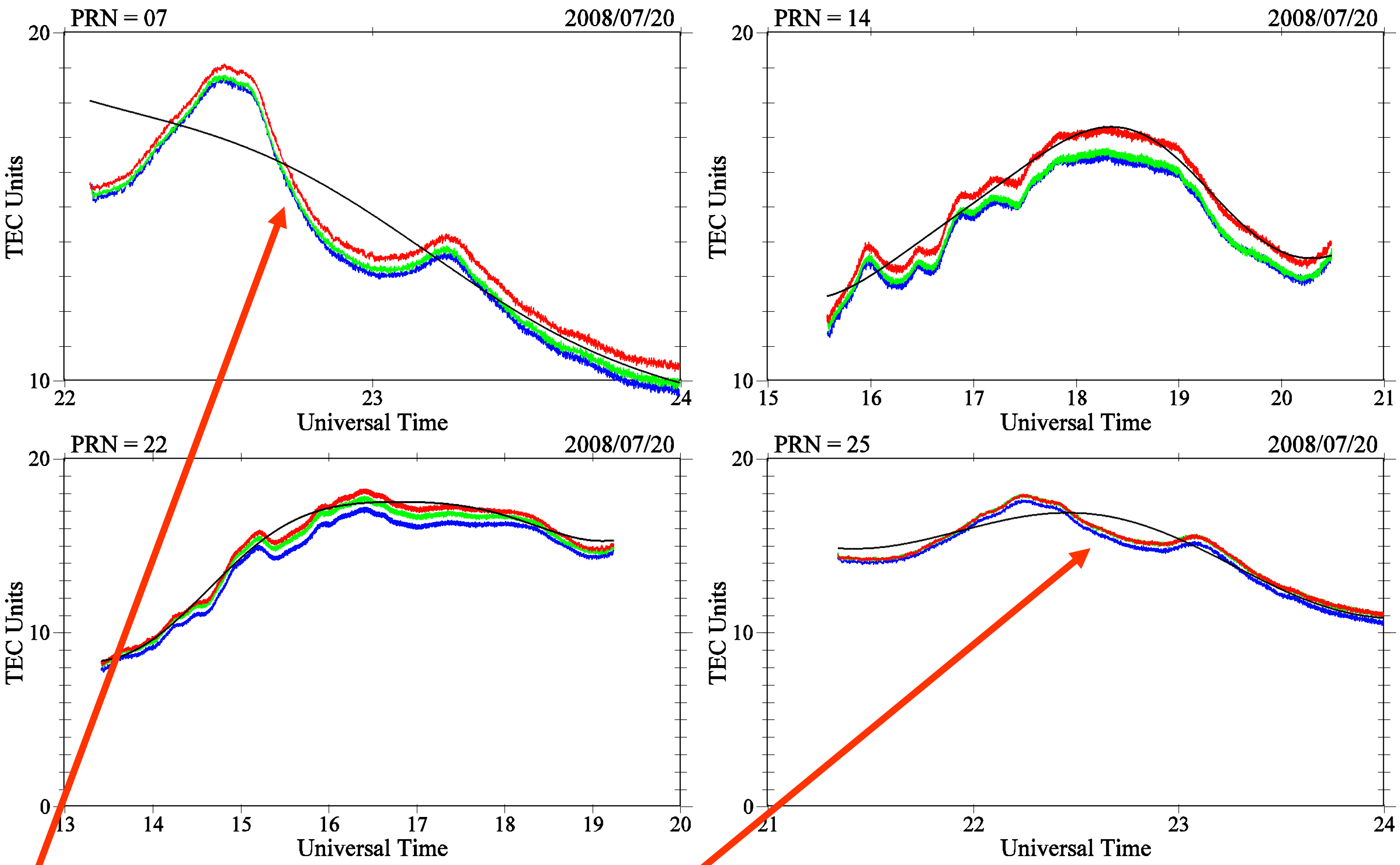

TEC perturbations associated with a TID that has a ~40 min period.

TEC perturbations for PRNs 22 and 32 recorded on July 20, 2008

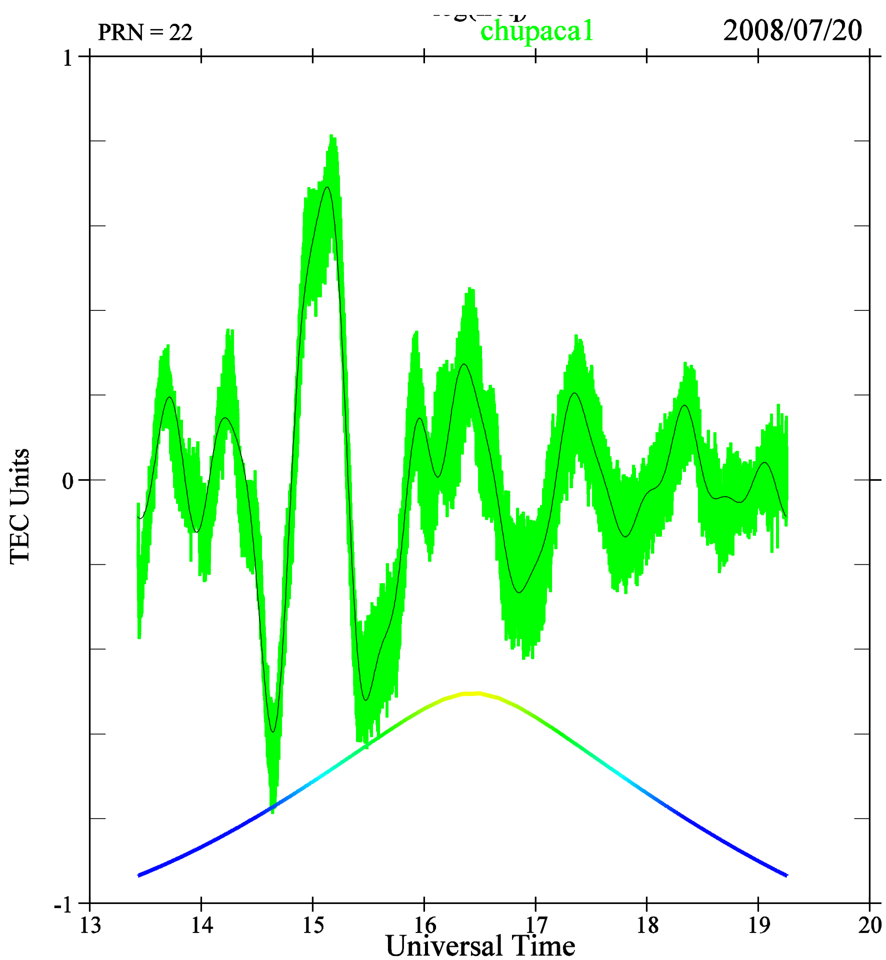

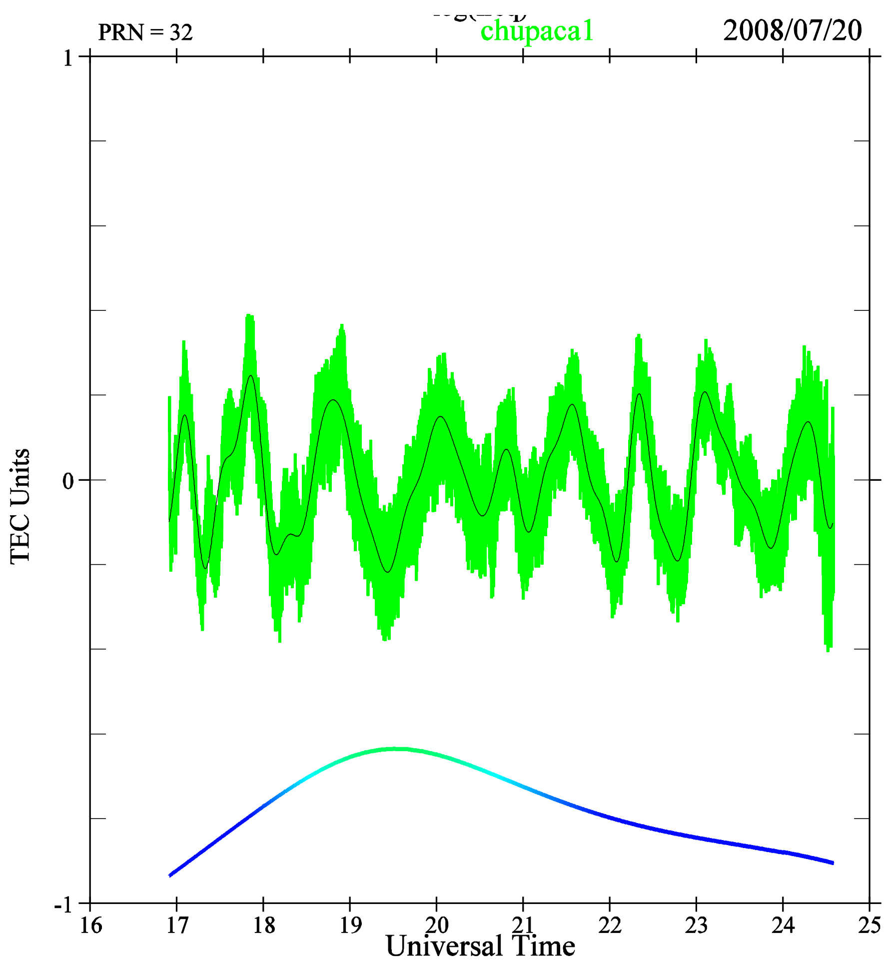

Cross-correlation method to calculate lag between dTEC traces

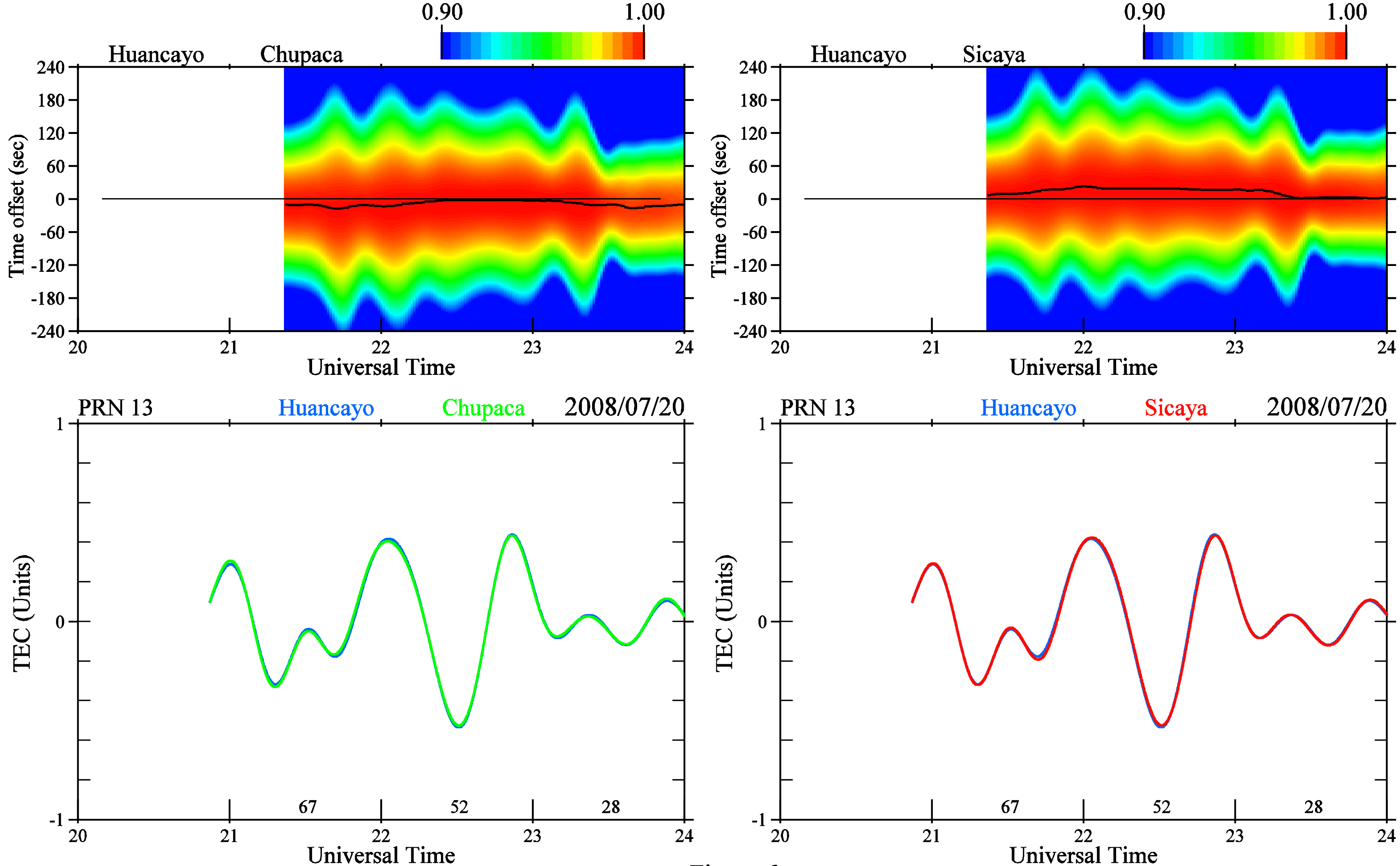

Figure 6

Phase Velocity ($V_h(t)$) and Direction of Propagation ($\alpha(t)$) of TID using measured time delays between Huancayo – Chupaca and Huancayo – Sicaya

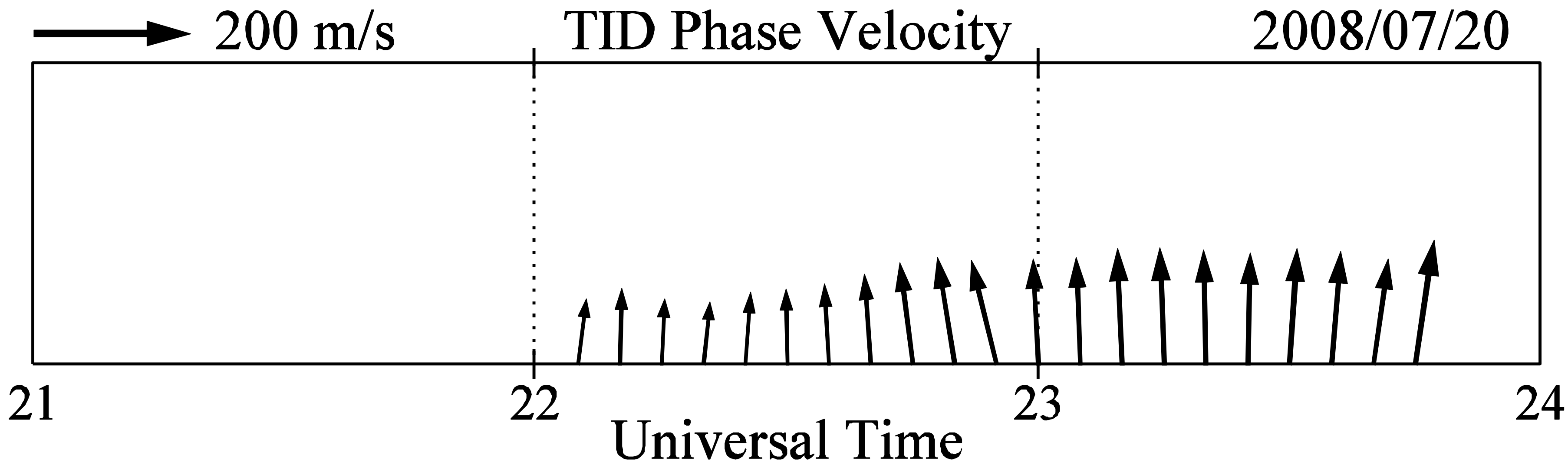

$\alpha(t) = arctan((Y_C T_{B\text{-}A} - Y_A T_{B\text{-}C})/(X_C T_{B\text{-}A} - X_A T_{B\text{-}C}))$

$V_h(t) = (Y_C \cos(\alpha(t)) - X_C \sin(\alpha(t)))/T_{B\text{-}C} + w_x(t) \sin \alpha(t) + w_y(t) \cos \alpha(t)$

$T_{B\text{-}A}$ and $T_{B\text{-}C}$ are the time delays between Huancayo – Sicaya and Huancayo – Chupaca. $w_x(t)$, and $w_y(t)$ are the x and y projections of the sub-ionospheric intersection point velocity.

Maps of TIDs for July 20, 2008

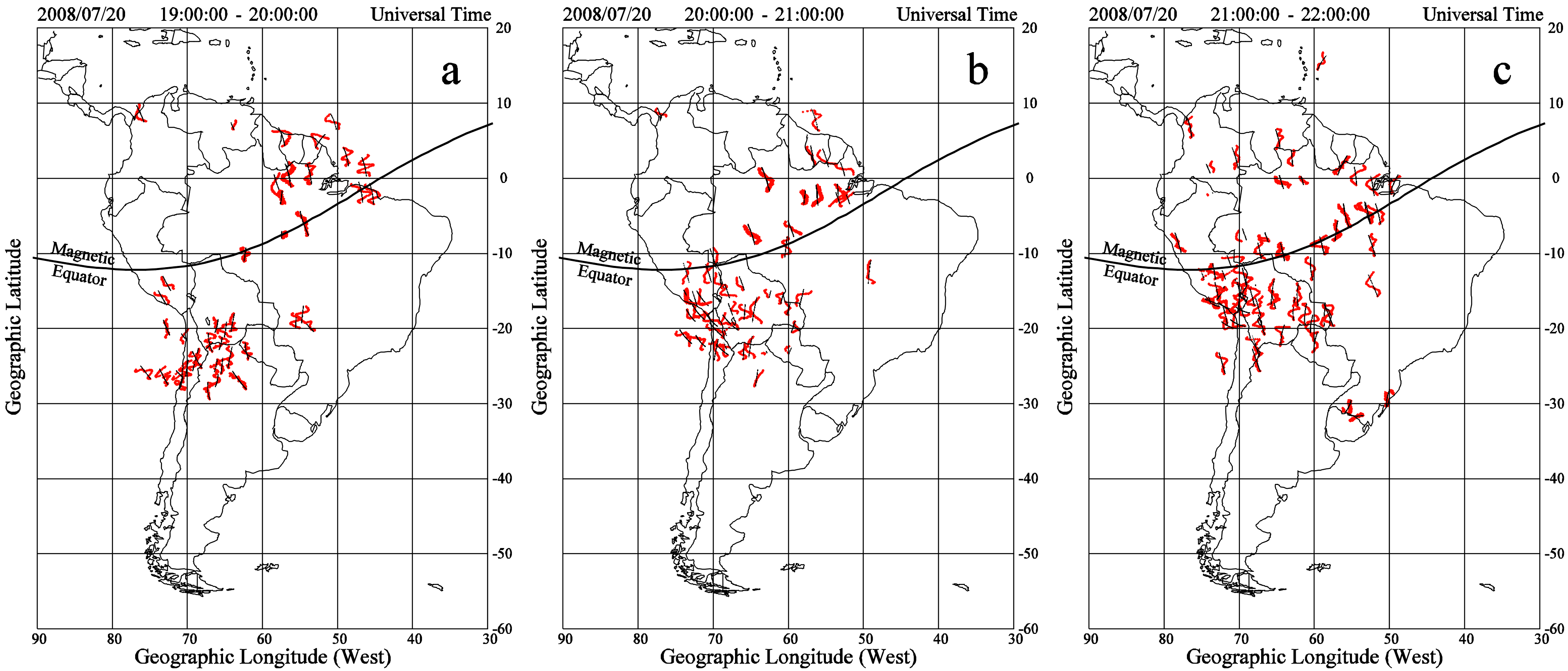

TEC perturbations observed in other stations on July 20, 2008

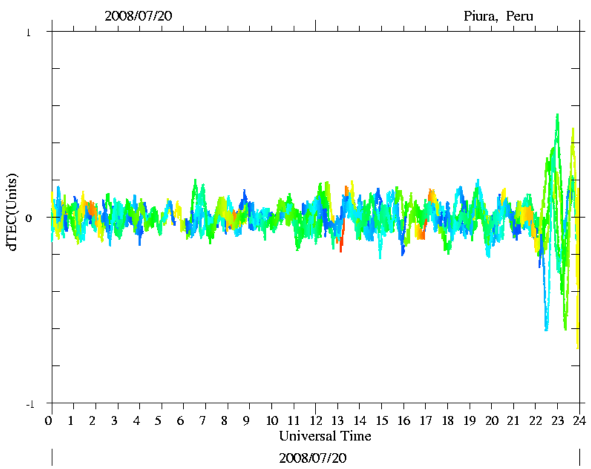

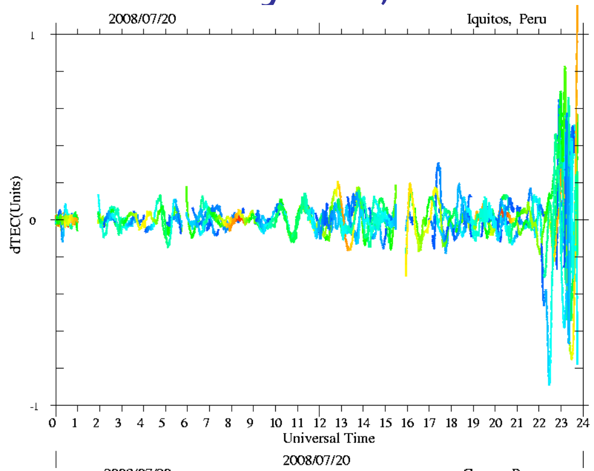

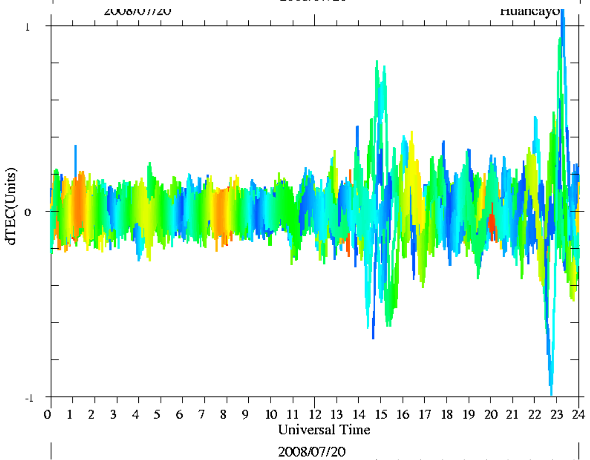

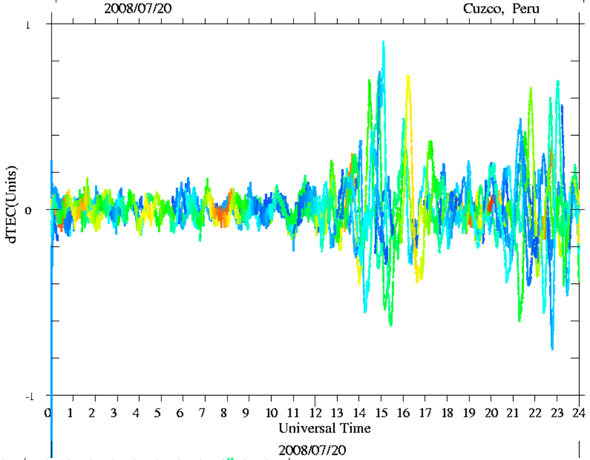

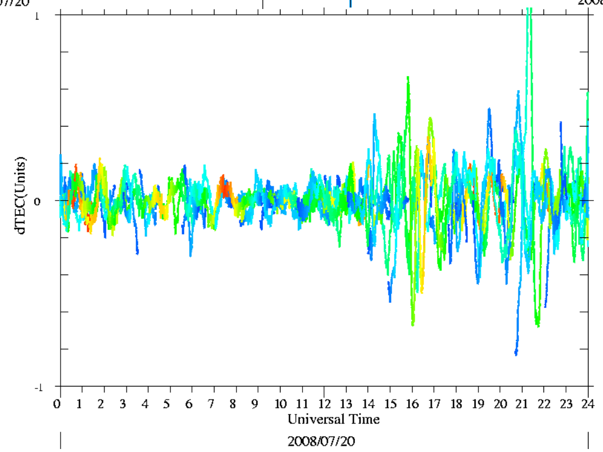

X-Correlation Functions for HYO – Cuzco and HYO - Piura

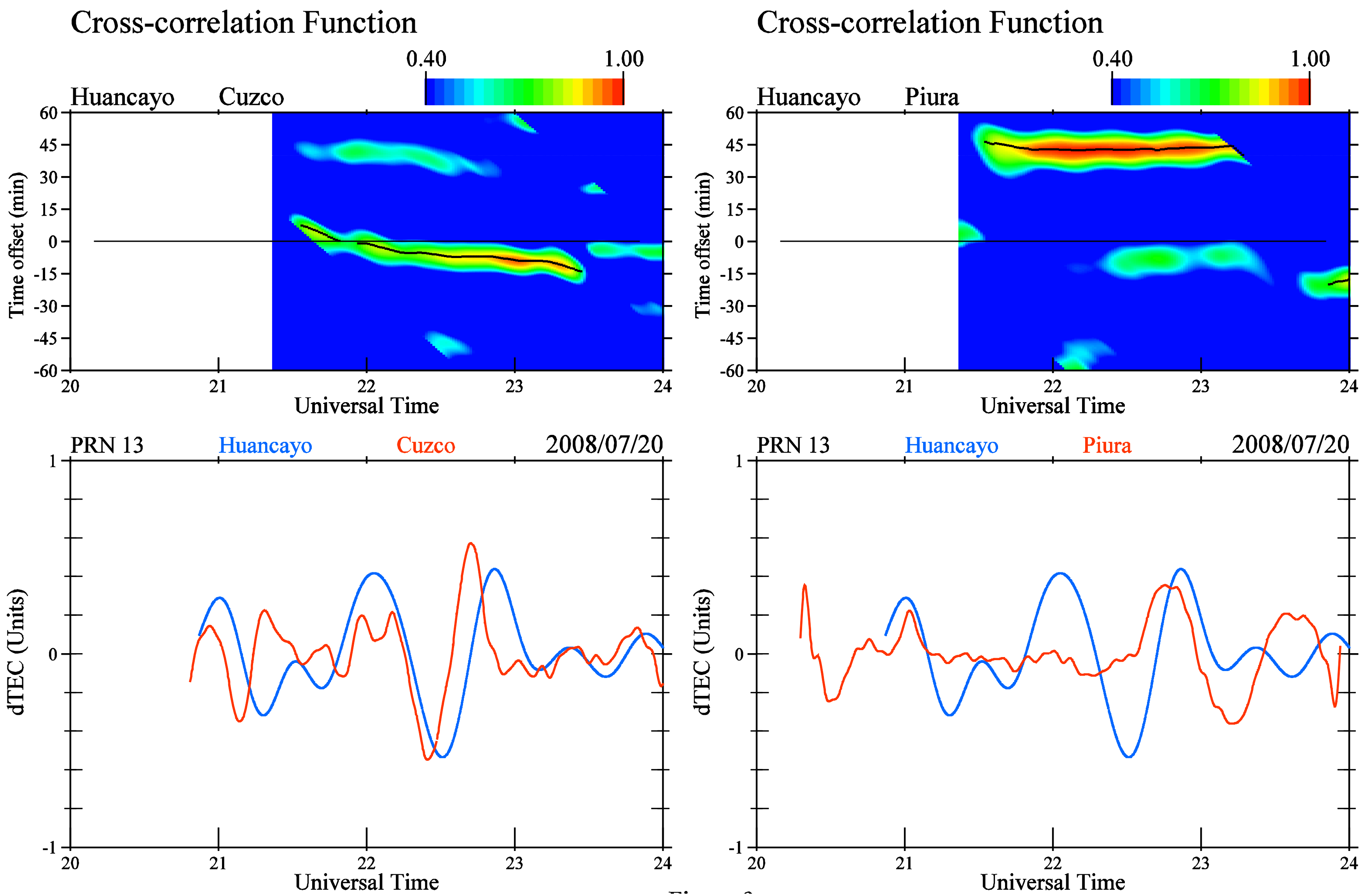

Comparison of TIDs Phase Velocities derived using the Small and the LISN networks

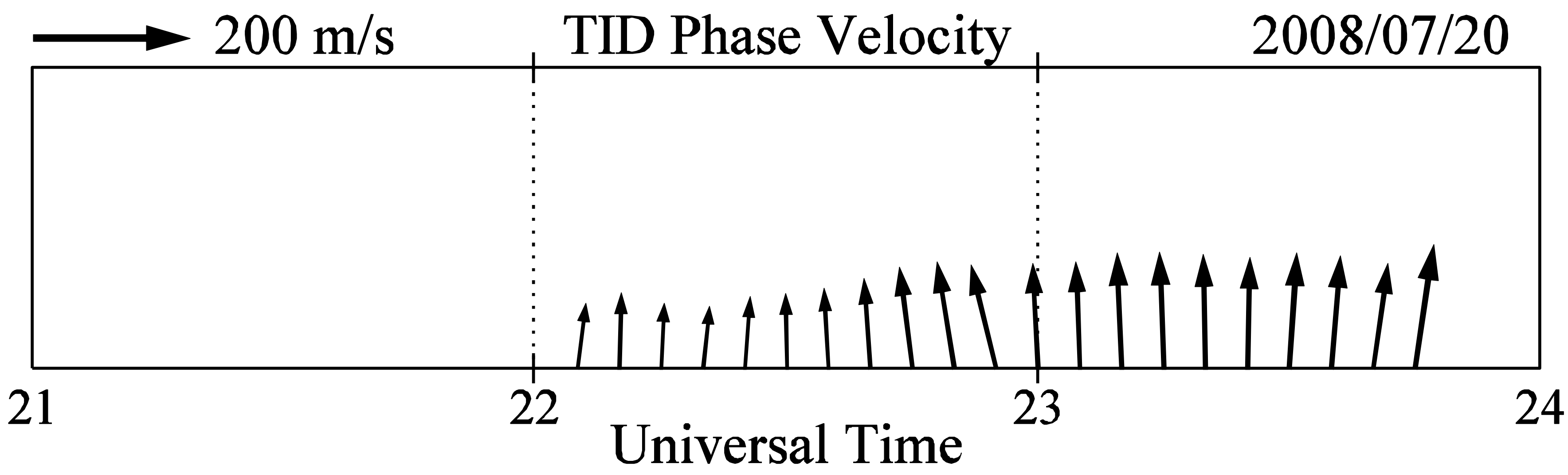

Huancayo - Cuzco - Piura

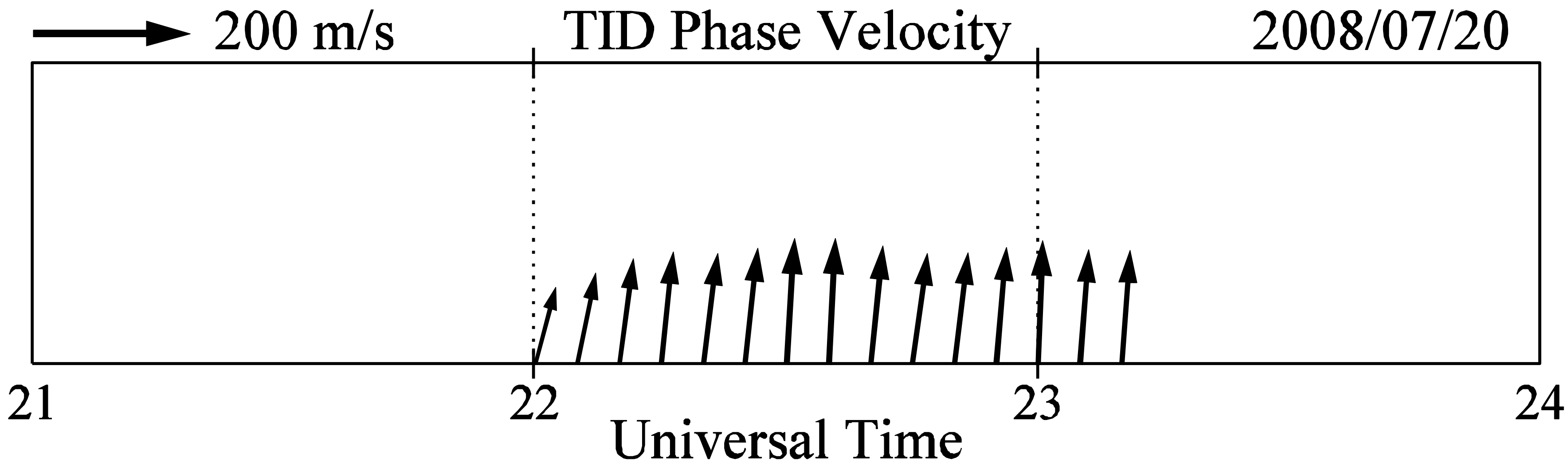

TID observations for September 01, 2008 (03 -04)

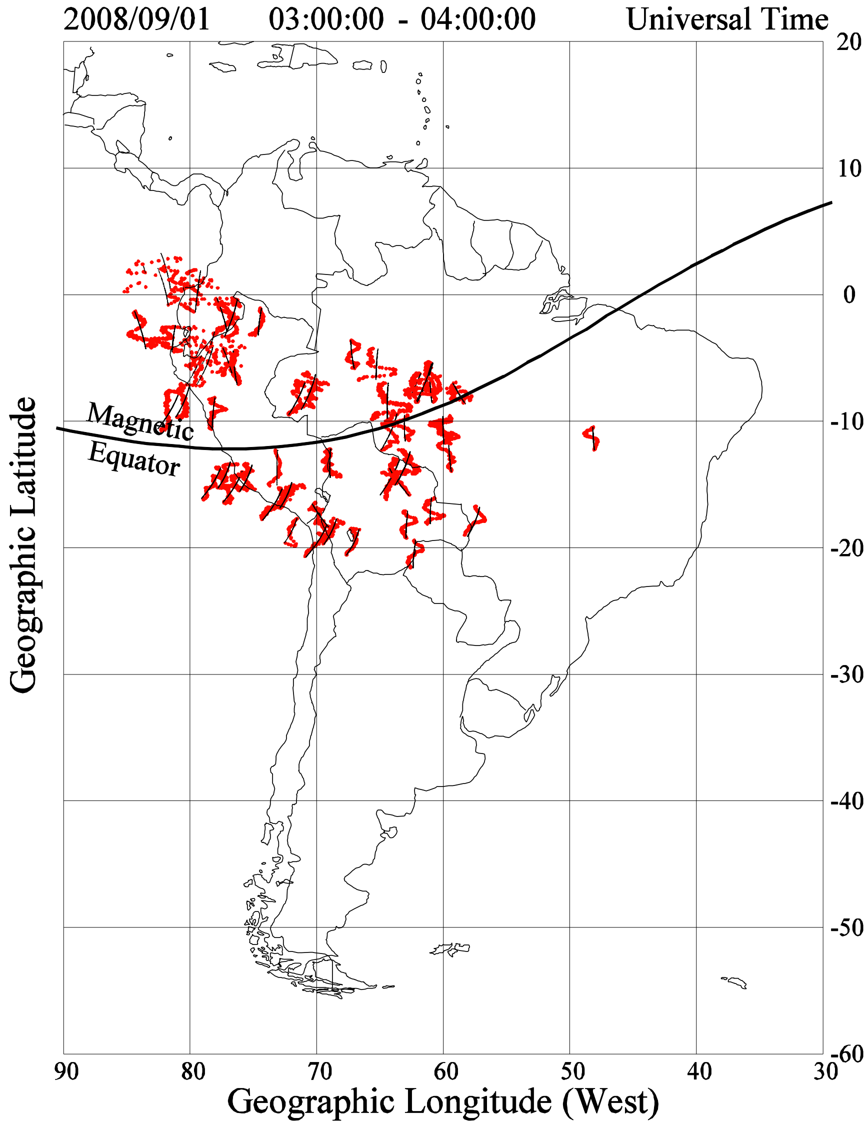

Infra-red Brightness Temperature for September 01, 2008 for 03 UT

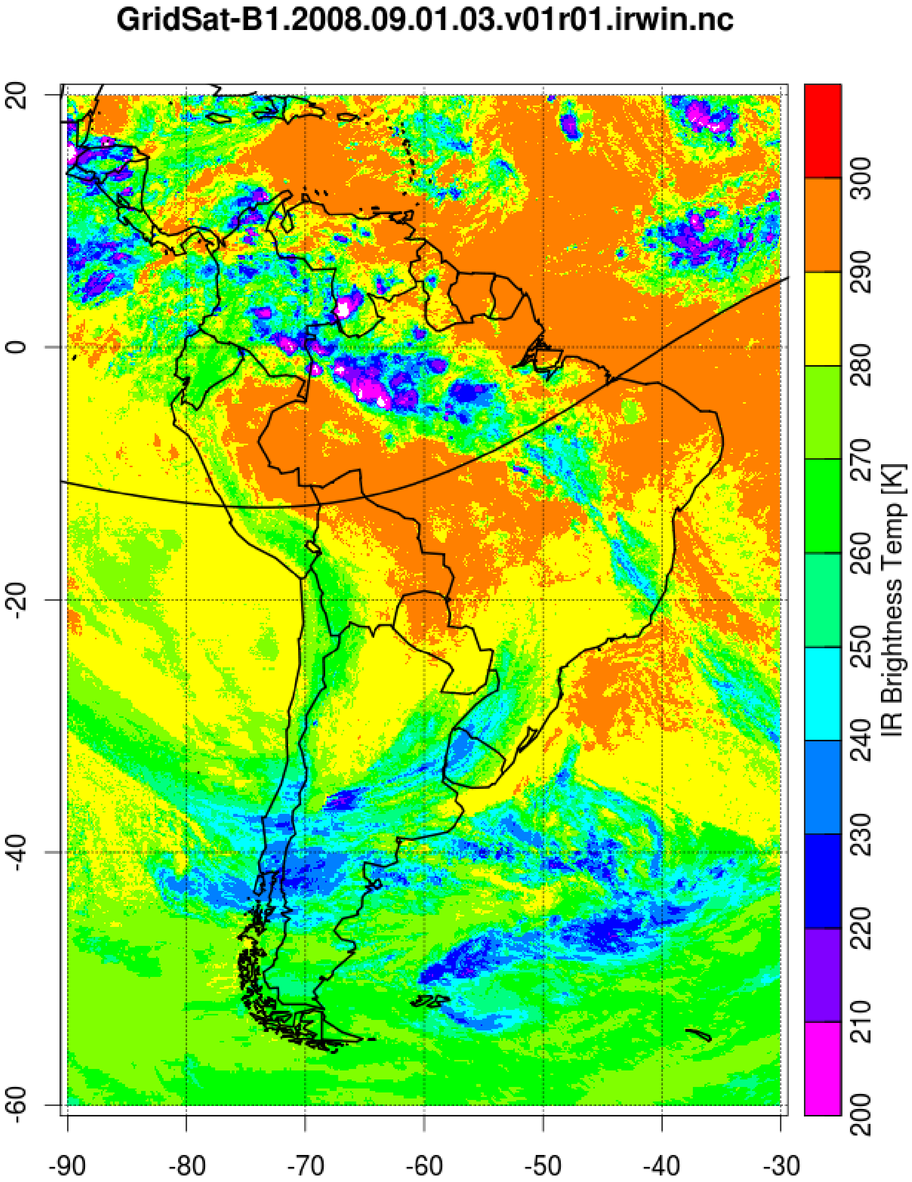

Provided by Kyle Weins

VIPIR Ionosonde

(Designed by Terry Bullett and Bob Livingston)

LISN Ionosonde

Vertical Incidence Pulsed Ionospheric Radar (VIPIR)

Designed for extreme performance and flexibility

8 Receiving Antennas – dipoles (4 N/S and 4 E/W)

4 Transmitting Antenna towers (Log periodic)

Operated at Jicamarca between 2008 and 2010.

Jicamarca Field Site

E Region and ESF

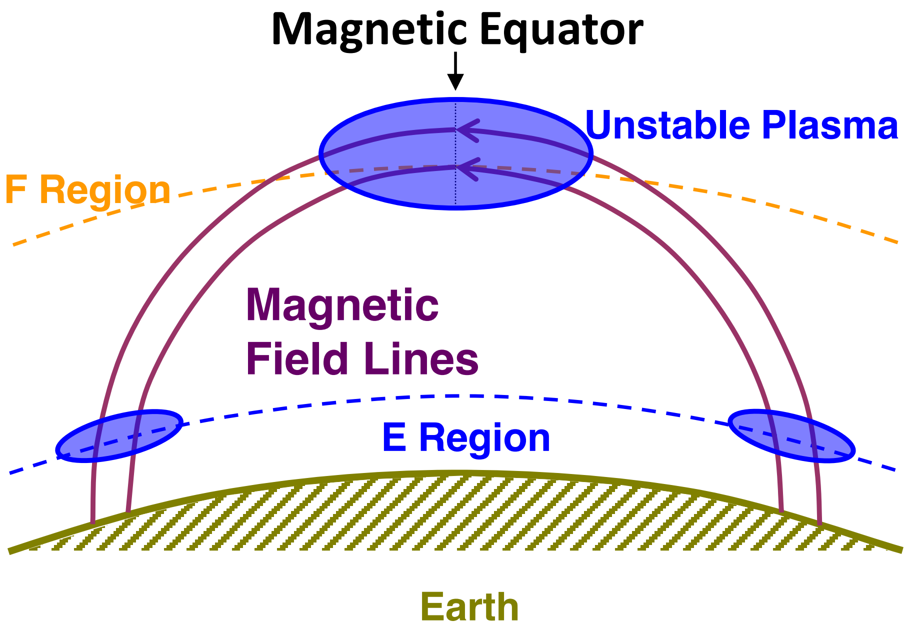

The field lines that intersect the E region over the cities of Sao Gabriel, Brazil and Tupiza, Bolivia map to between 295 – 320 km at the magnetic equator. We will be able to investigate: (1) if E_s layers short out ESF. (2) role of equatorial and off-equatorial E region to balance pre-reversal currents.

Provided by K. Groves

SA Ionosondes (partial)

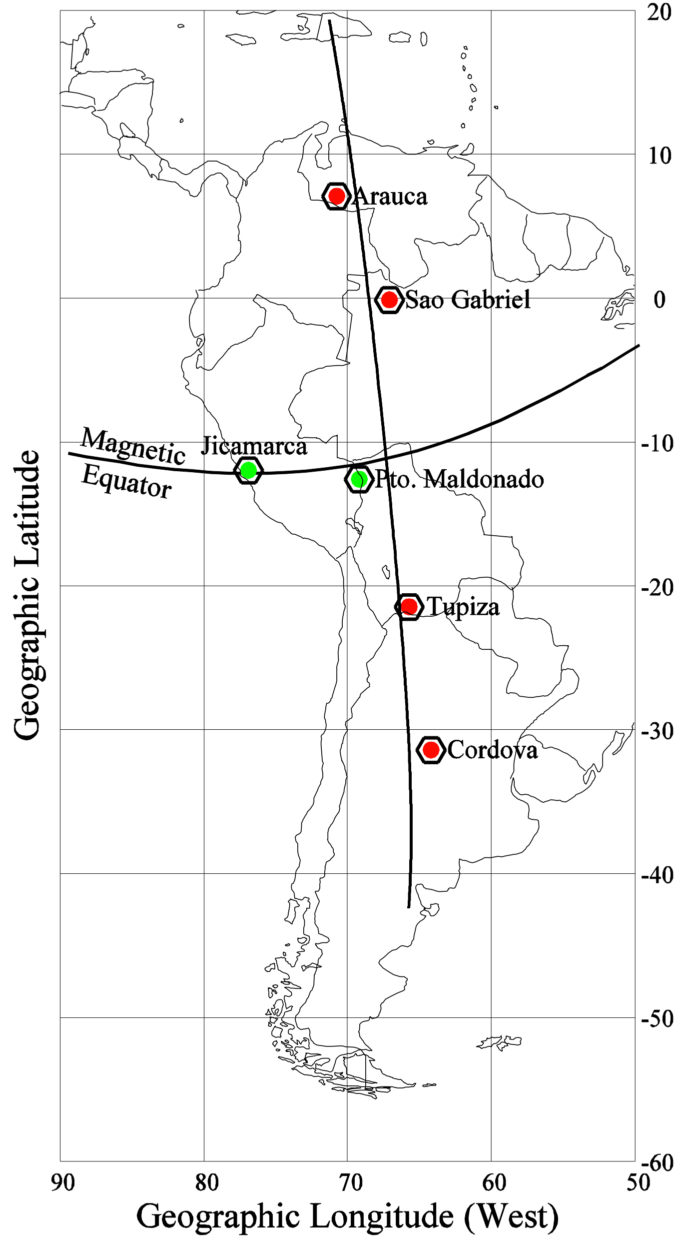

Field-line Mapping from the E regions (100 km) of Sao Gabriel do Cachoeira and Tupiza to the Magnetic Equator

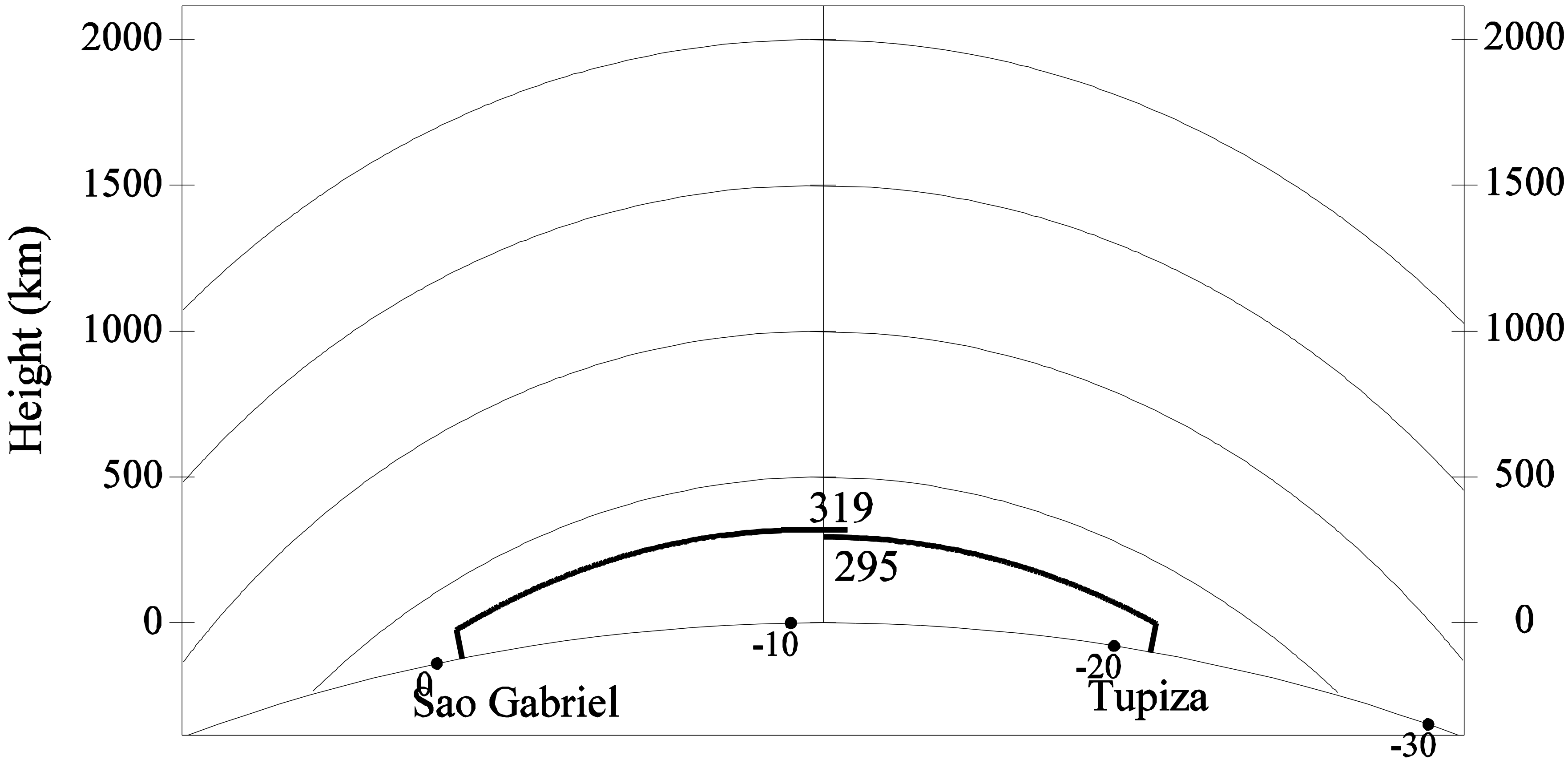

Projects to be conducted with VIPIR ionosondes

To use VIPIR measurements of E and E_s layers provided by two ionosondes placed at nearly conjugate locations, ~11-12 on both sides of the magnetic equator, and to study the role of E_s layers on the onset and dynamics of ESF.

To calculate the value of the meridional winds using the LISN ionosondes and compare these values with measurements conducted in South America using Fabry-Perot interferometers and other techniques.

To use data from GPSs and VIPIRs and numerical techniques to calculate plasma density profiles along the LISN meridian (~67 W).

Compare F_of_2 values from P. Maldonado at the magnetic equator and Jicamarca also at the mag. eq, but separated by 800 km to observe longitudinal variability.

LISN VIPIR Database

http://lisn.igp.gob.pe/ionosonde

- Daily files
  - NCDF
  - IDL SAVE file
- On-line plots
  - Power ionograms (O and X modes)

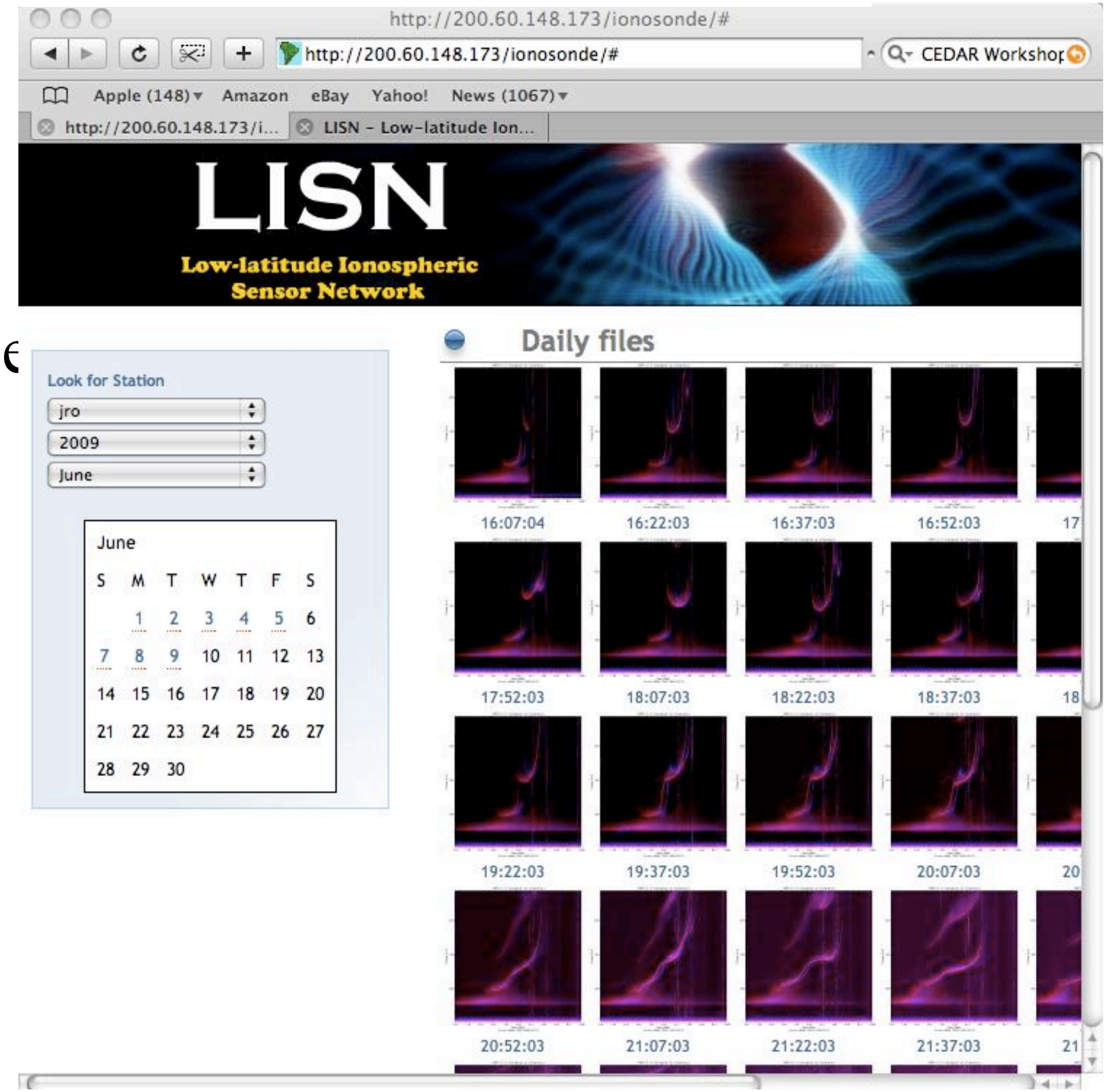

Ionogram recorded on Sept 19, 2009 at JRO

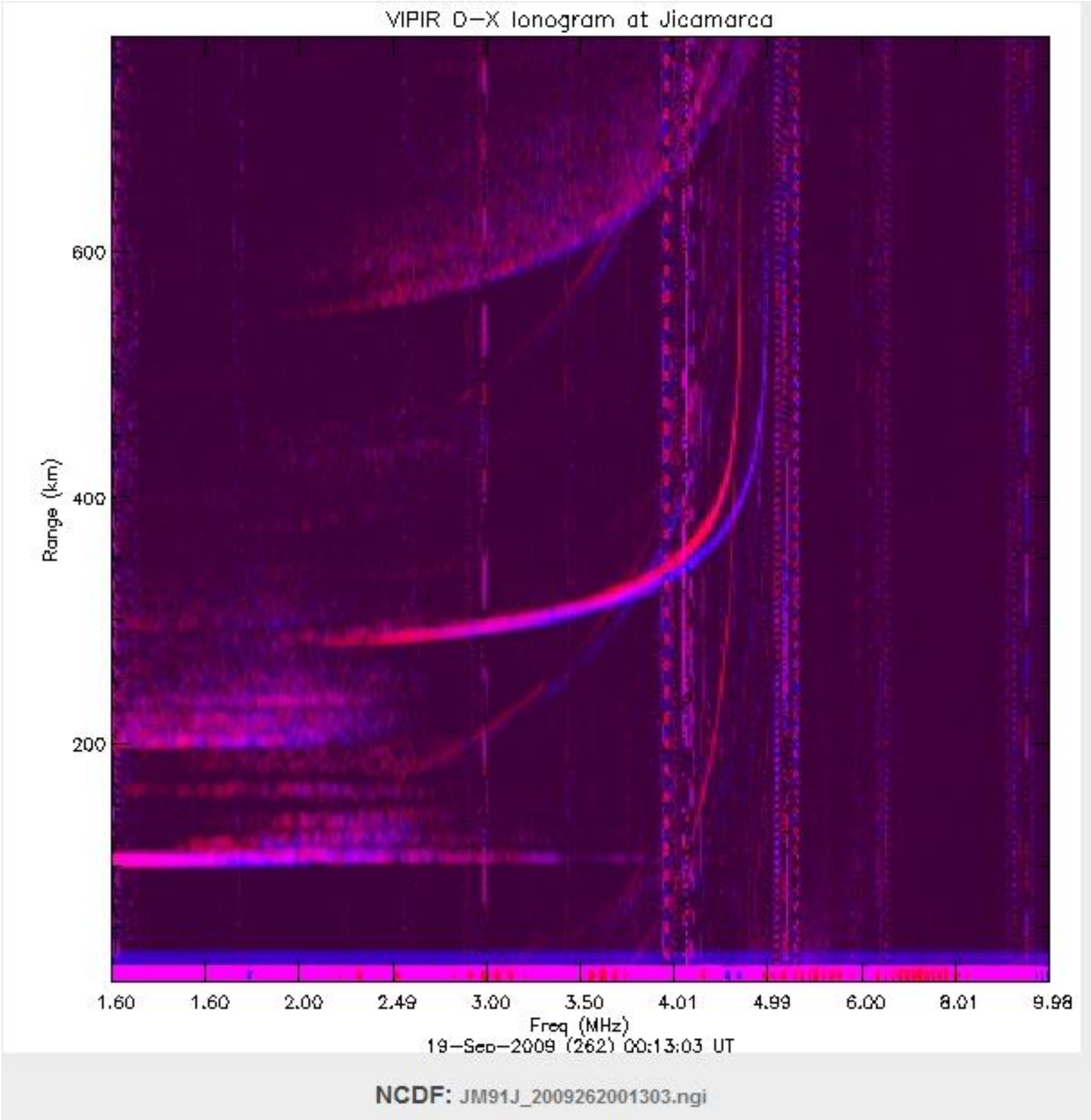

Multiple E_s traces

Why the VIPIR ionosonde was selected for LISN

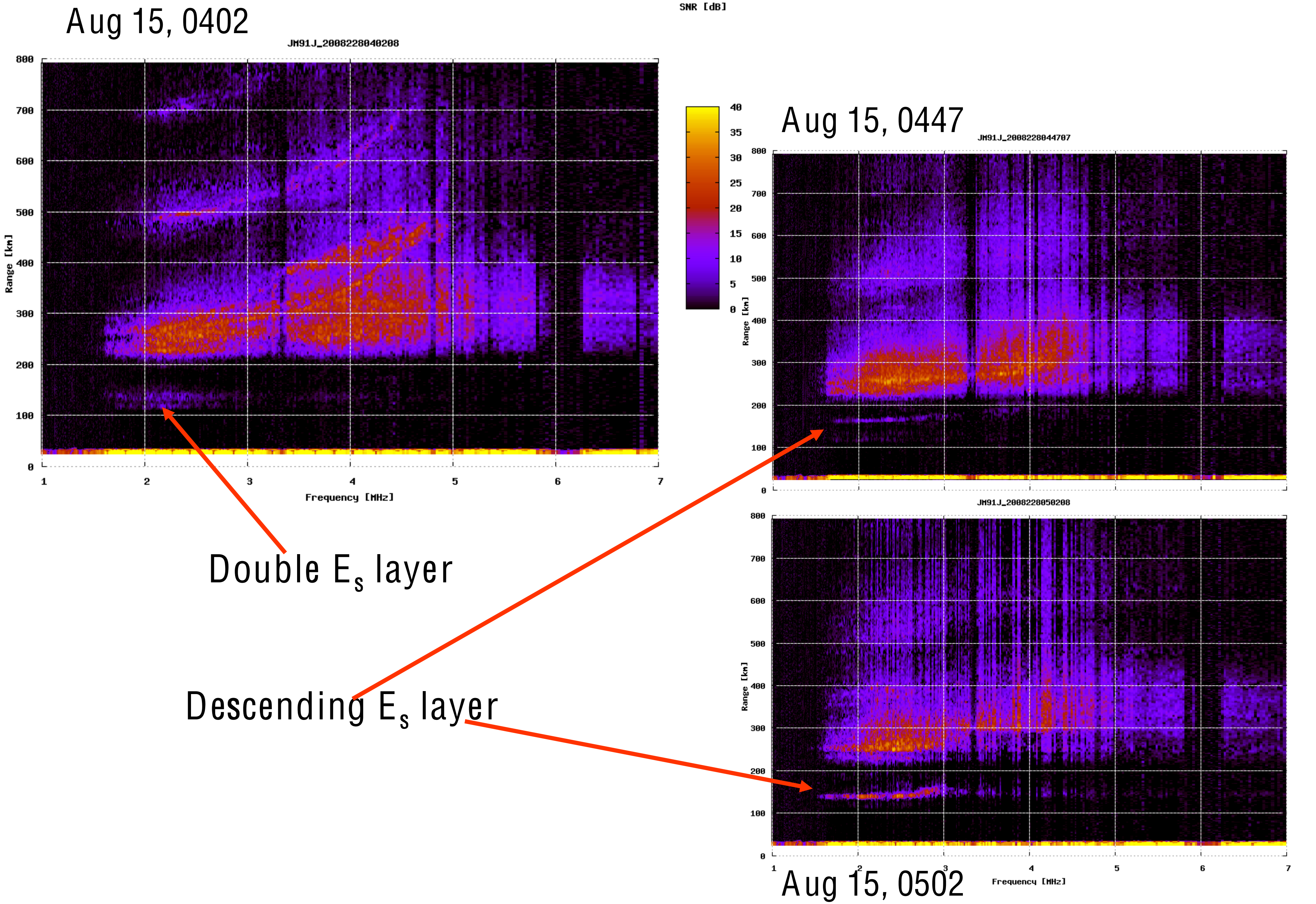

Real –Time calculation of densities using ESIR

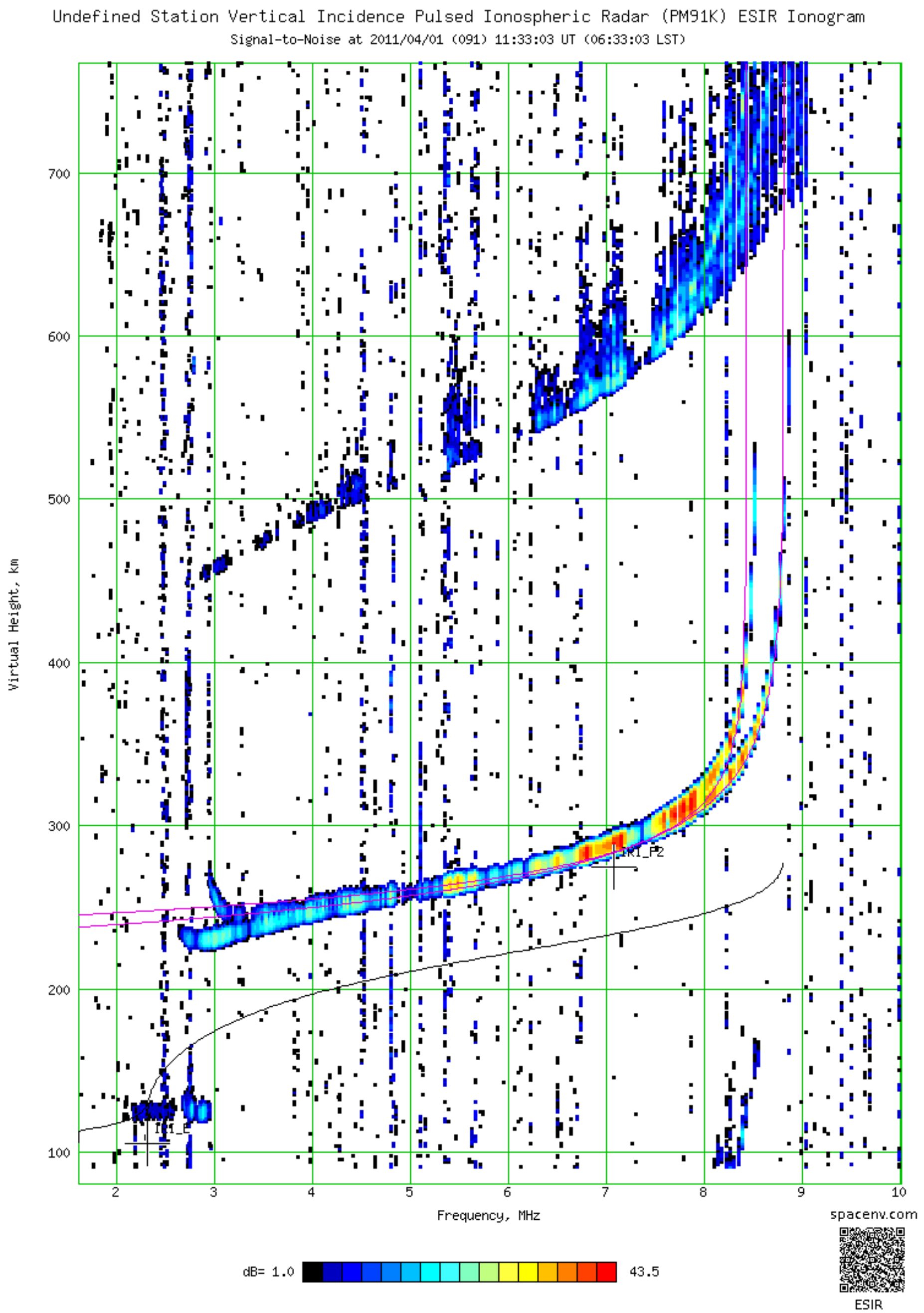

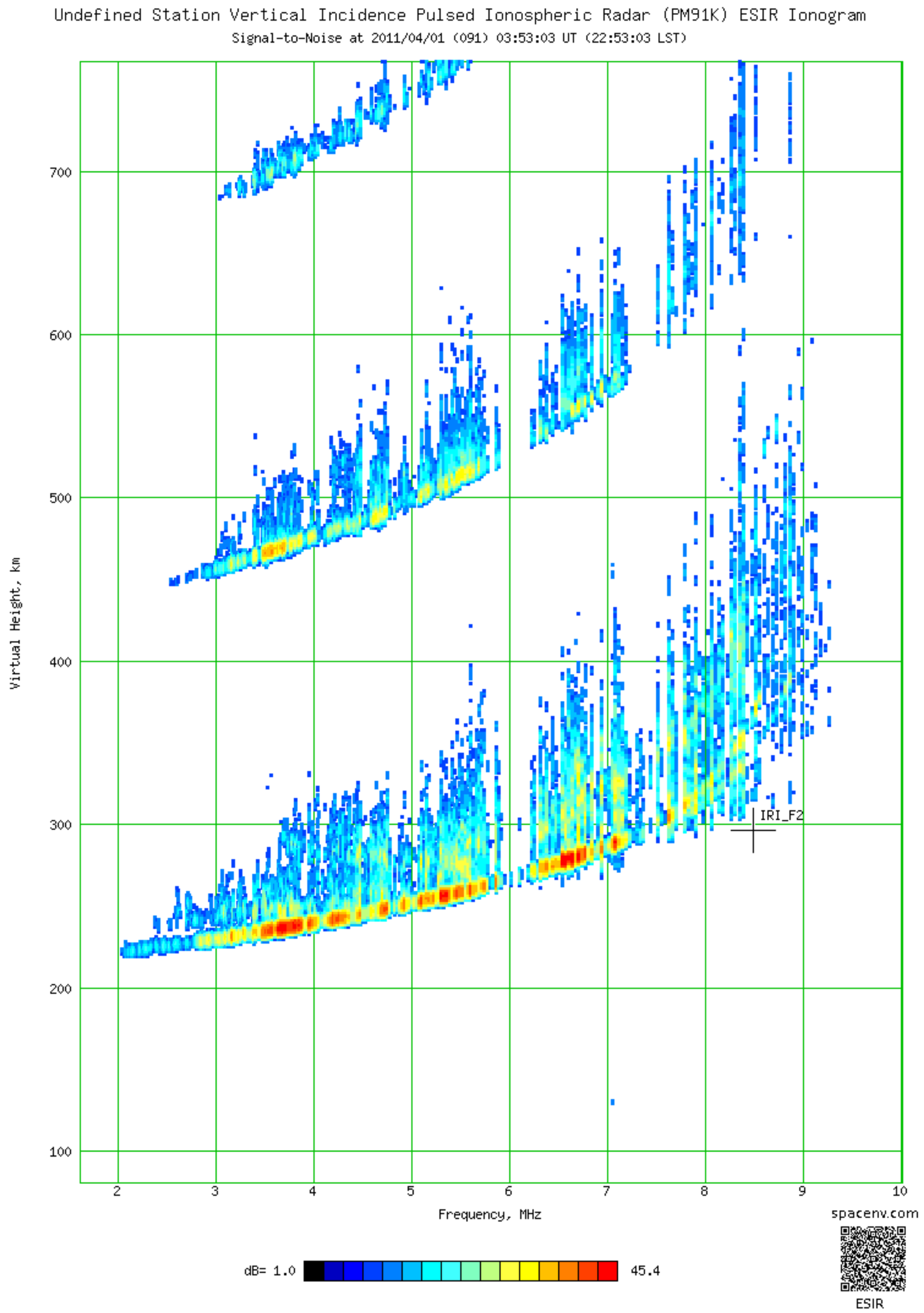

Meridional chain of the South-East Asia Low-latitude Ionospheric Network (SEALION)

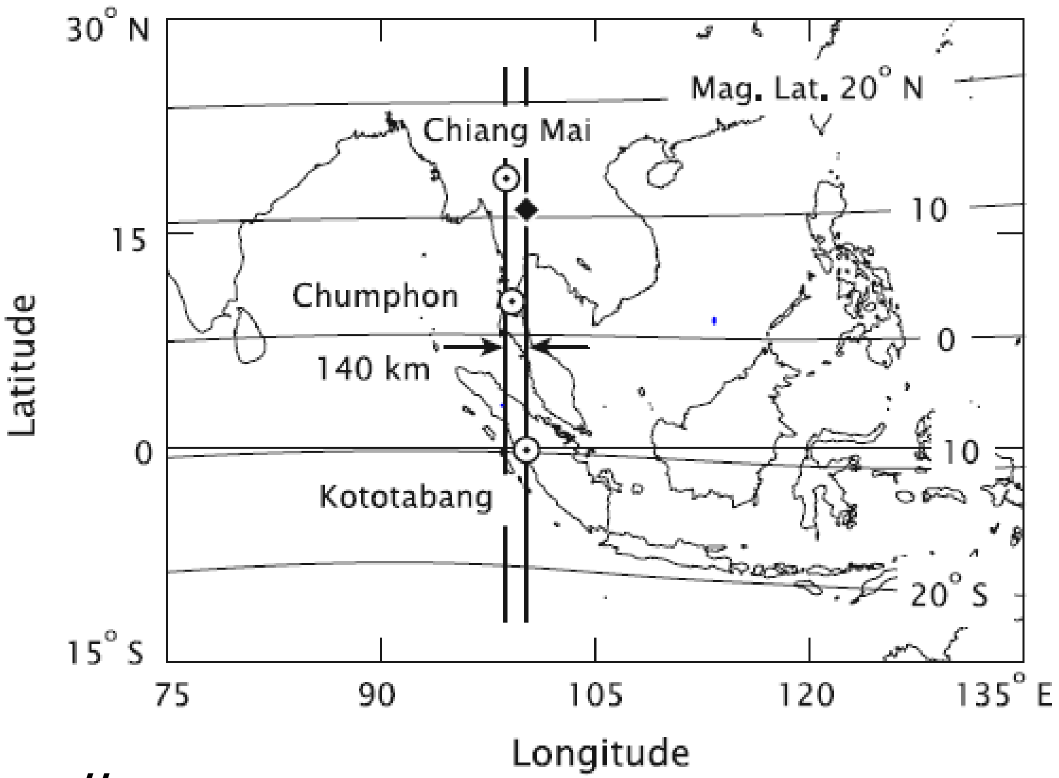

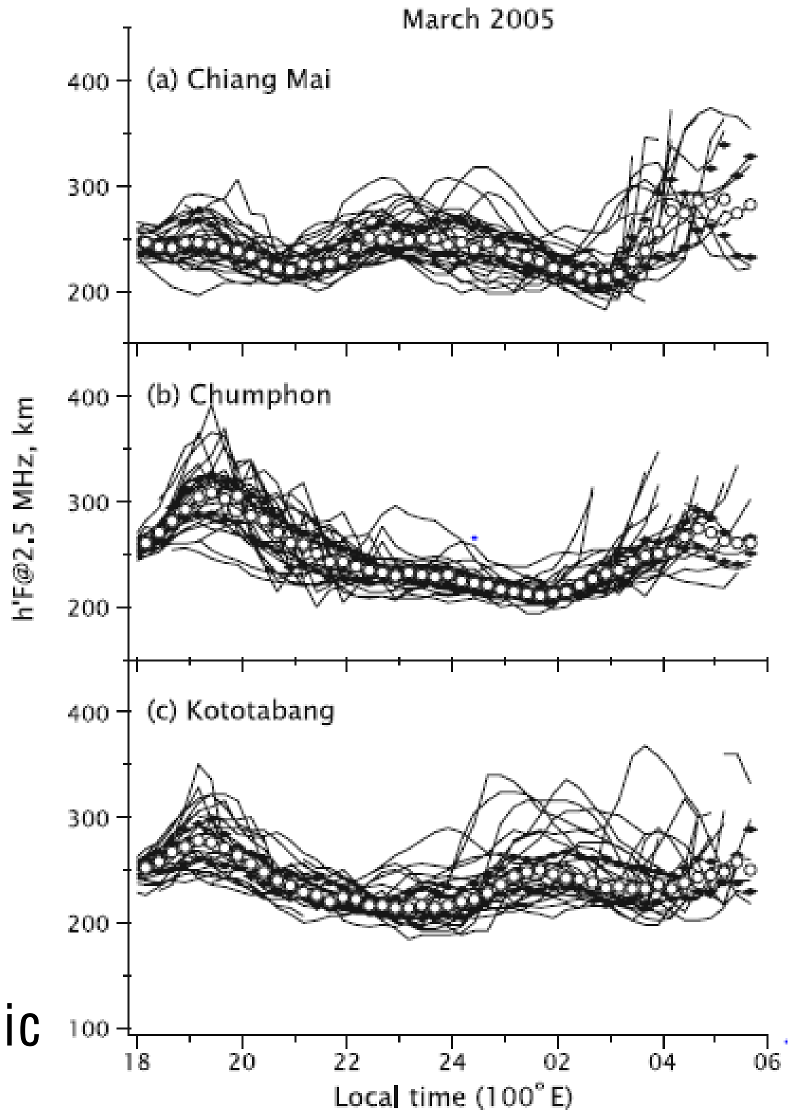

$$\frac{dh_m}{dt} = D_{diff} + V_z \cos I + U_M \cos I \sin I$$

h_m is the height of F region, D_{diff} is the diffusion term that depends on thermospheric conditions, V_z is the vertical velocity at the equator, U_M is the meridional wind, and I the dip angle.

Maruyama et al., 2008

Jicamarca - Pto. Maldonado foF2 comparison

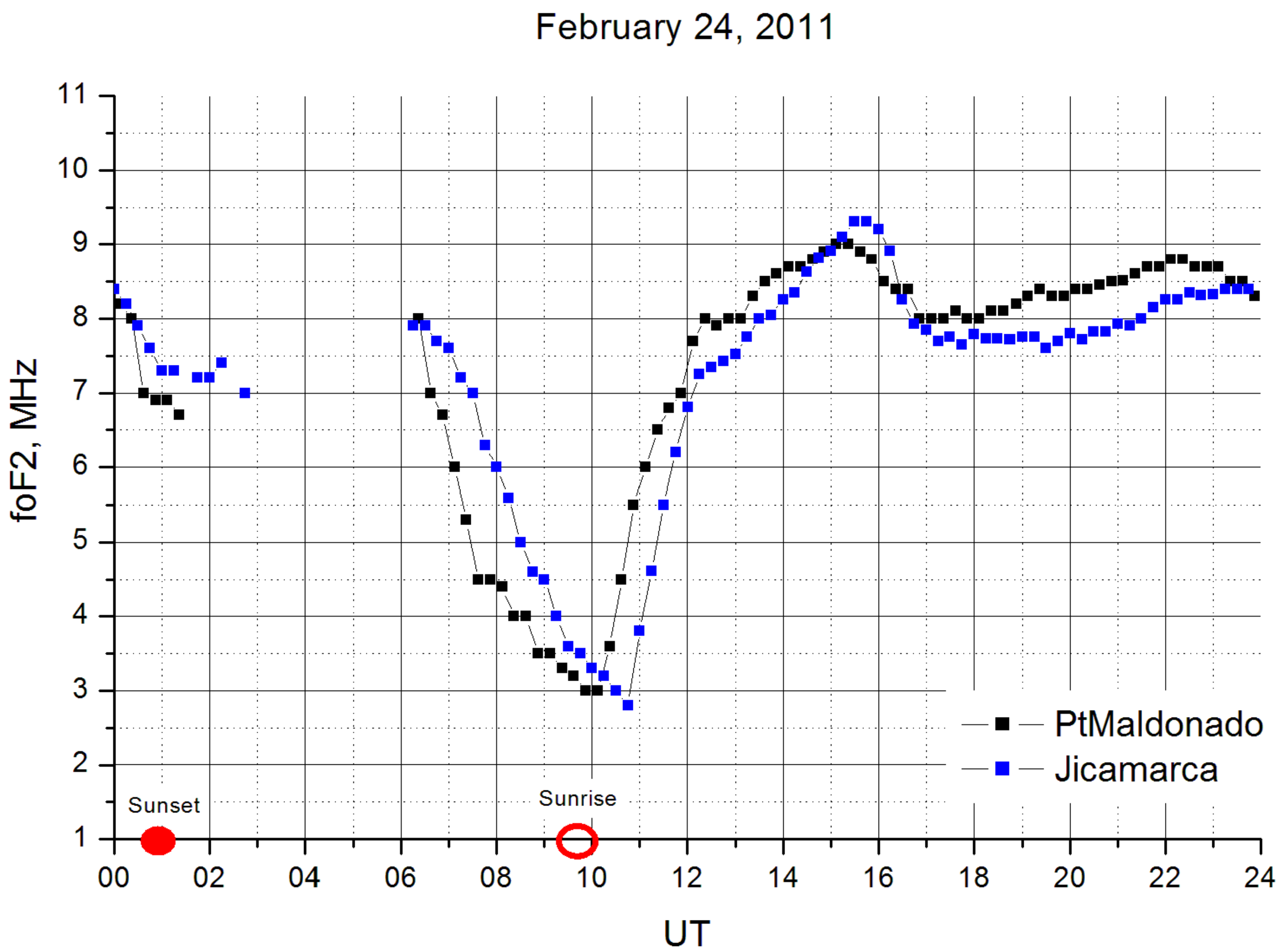

Development of new Magnetometer

- Overall Range: +/- 60,000nT.
- Dynamic Range: +/- 2000nT
- Resolution : 0.1nT
- Output: +/-2.5 VDC (analog signal)
- Digital outputs: USB, 5 output channels, X,Y,Z and 2 temperature sensors
- Internet data rate: 5min.

- Sensor : Triaxial ring core fluxgate.
- Sensor Module: PVC cylinder de 4" x 0.80 m, contains internal temperature sensor.
- Electronic unit: AGC, fields cancellation and filters, including a data logger of high resolution : 20 bits, 8 channels, USB.

4 Magnetometer Baselines in SA; LISN (Green)

4 Magnetometer Baselines in SA; LISN (Green) and Others (blue)

Solar Energy Budget (from Kerri Cahoy's ISEA-12)

Why is latent heat important?

Latent heat transitions nearly a quarter of Earth's incoming solar energy from the surface back to the atmosphere.

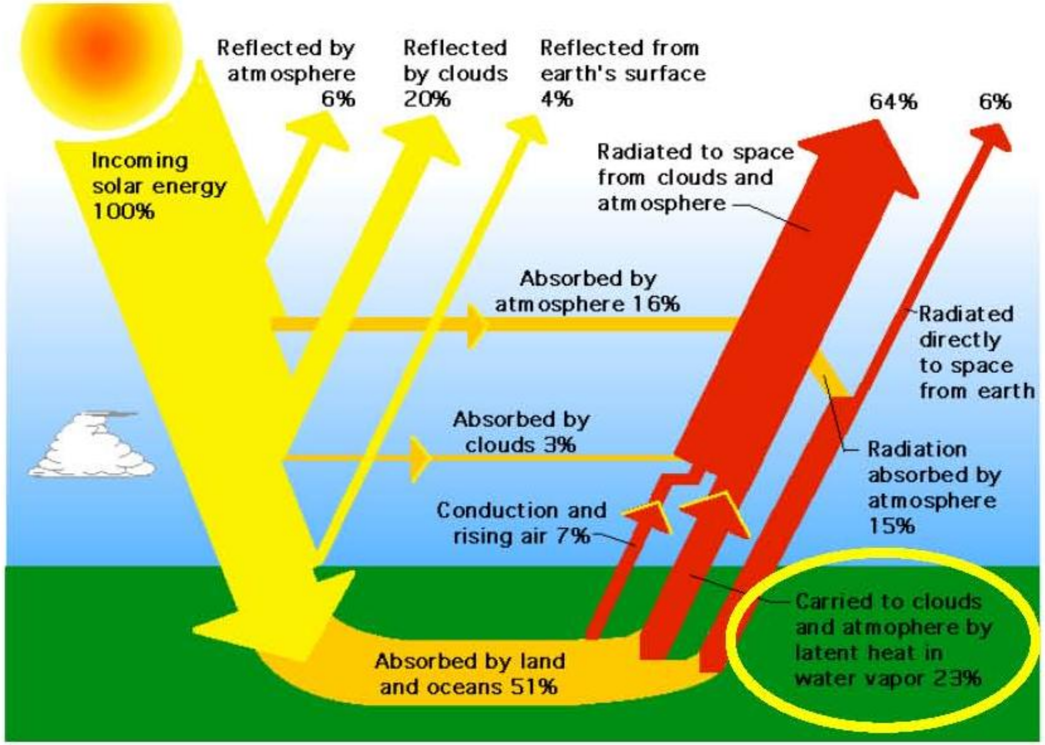

Graphic courtesy http://asd-www.larc.nasa.gov/erbe

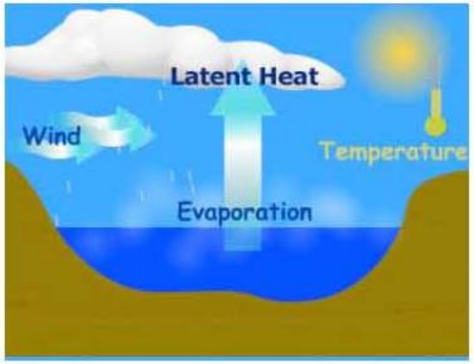

Can we use GPS RO profiles of **T**, **P**, and refractivity to relate to latent heat?

To what extent does change in the distribution of tropospheric latent heat map to ionospheric structure?

Notes: other factors also affect tidal structure, such as planetary and gravity waves.

Diurnal, eastward propagating, non-migrating (DE3) tides are thought to originate in the troposphere through latent heat release and to be responsible for the 4-cell, non-migrating structures observed in the **equatorial ionosphere… Observations of the 4-**cell structures

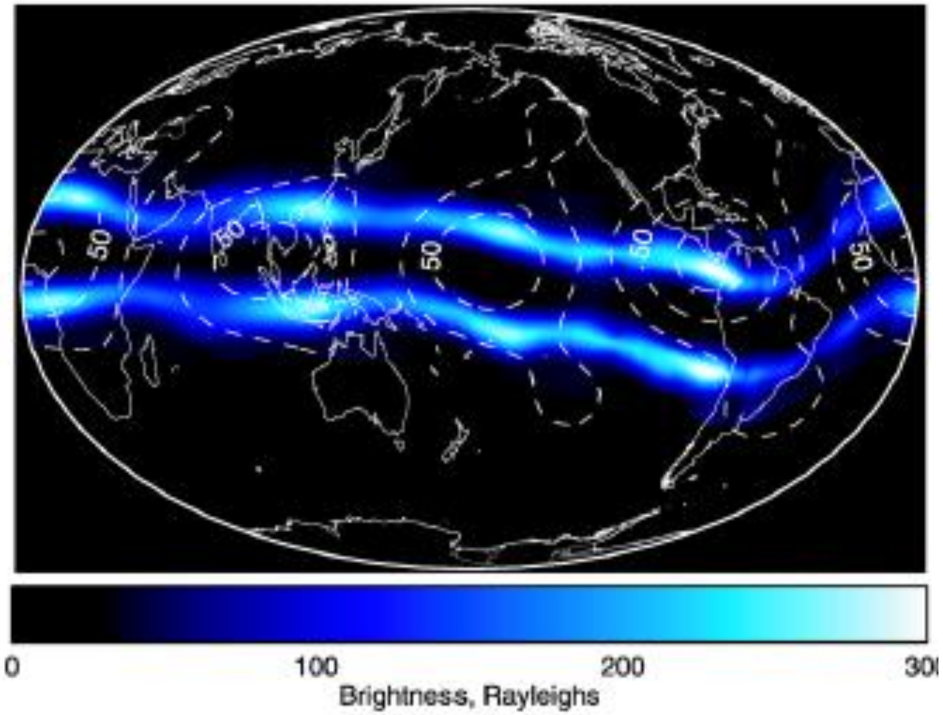

Nighttime IMAGE 135.6 nm radiances from O+ radiative recombination (Immel et al., 2006)

IMAGE = Imager for Magnetopause-to-Aurora Global Exploration.

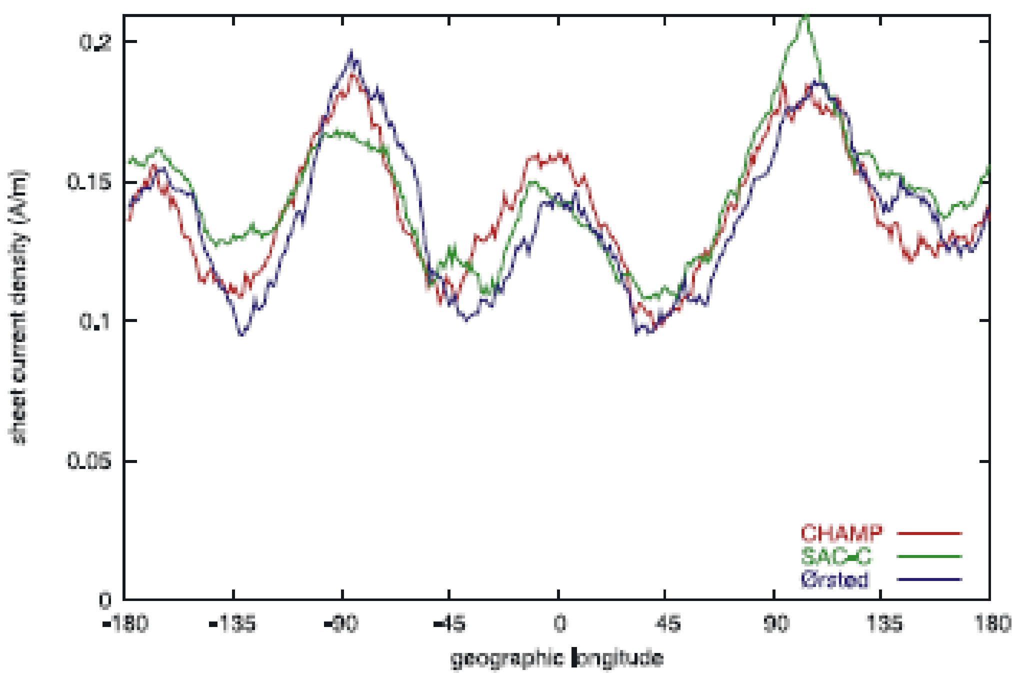

Noontime, magnetometer-observed equatorial electrojet current density vs longitude from CHAMP, SAC-C and Oersted satellites (England et al., 2006)

The steep longitude gradient in E B drift velocity at the cell boundary in the Peruvian sector

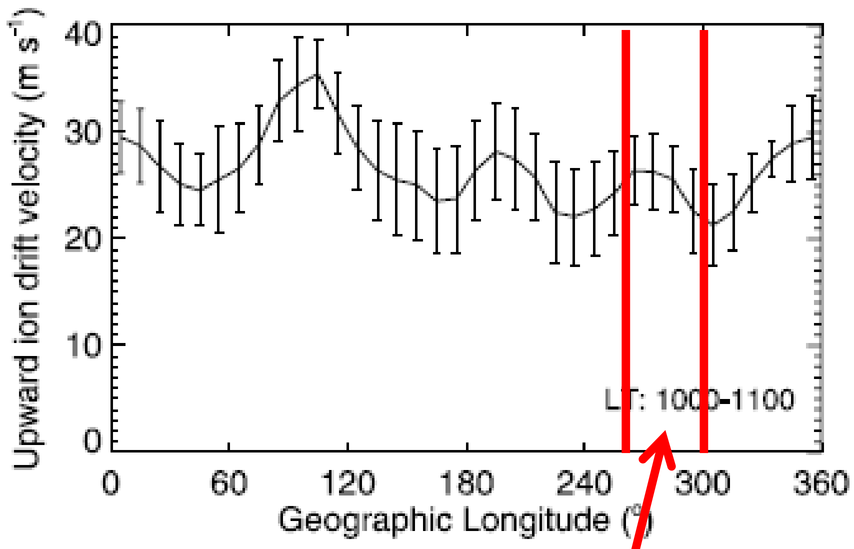

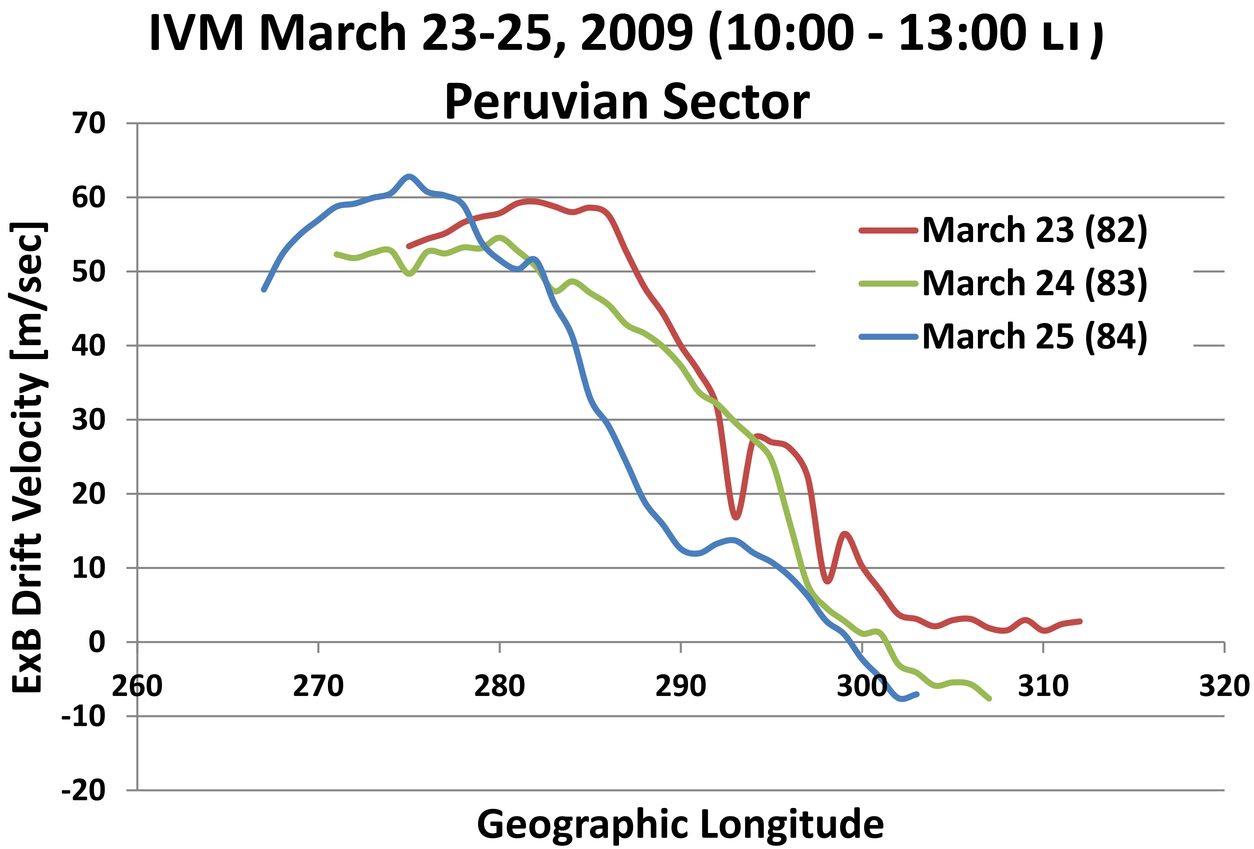

Sector included in lower plot (270 thru 310)

Longitude gradient in ExB drift ~ - 4 m/sec/degree

Provided by D. Anderson

All 3 days have equivalent slopes and they delineate the increase in ExB drift velocity across the Atlantic sector

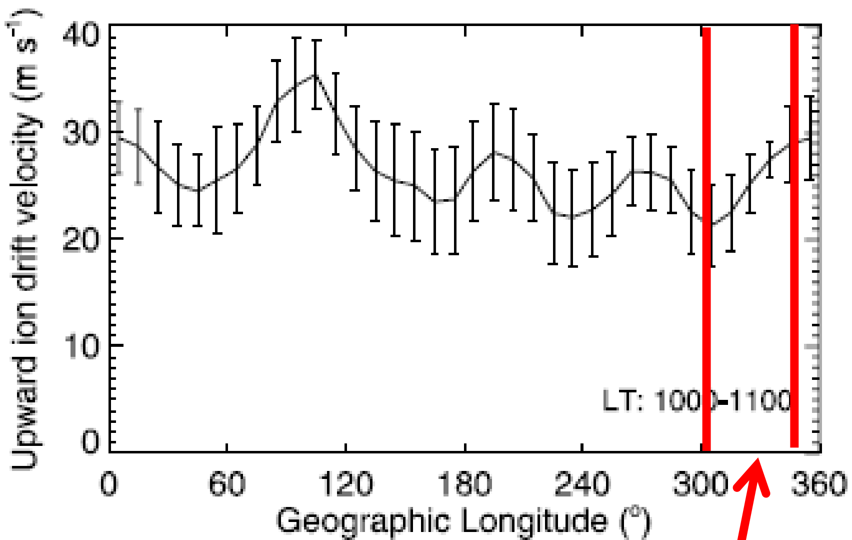

Sector included in lower plot (300 thru 350)

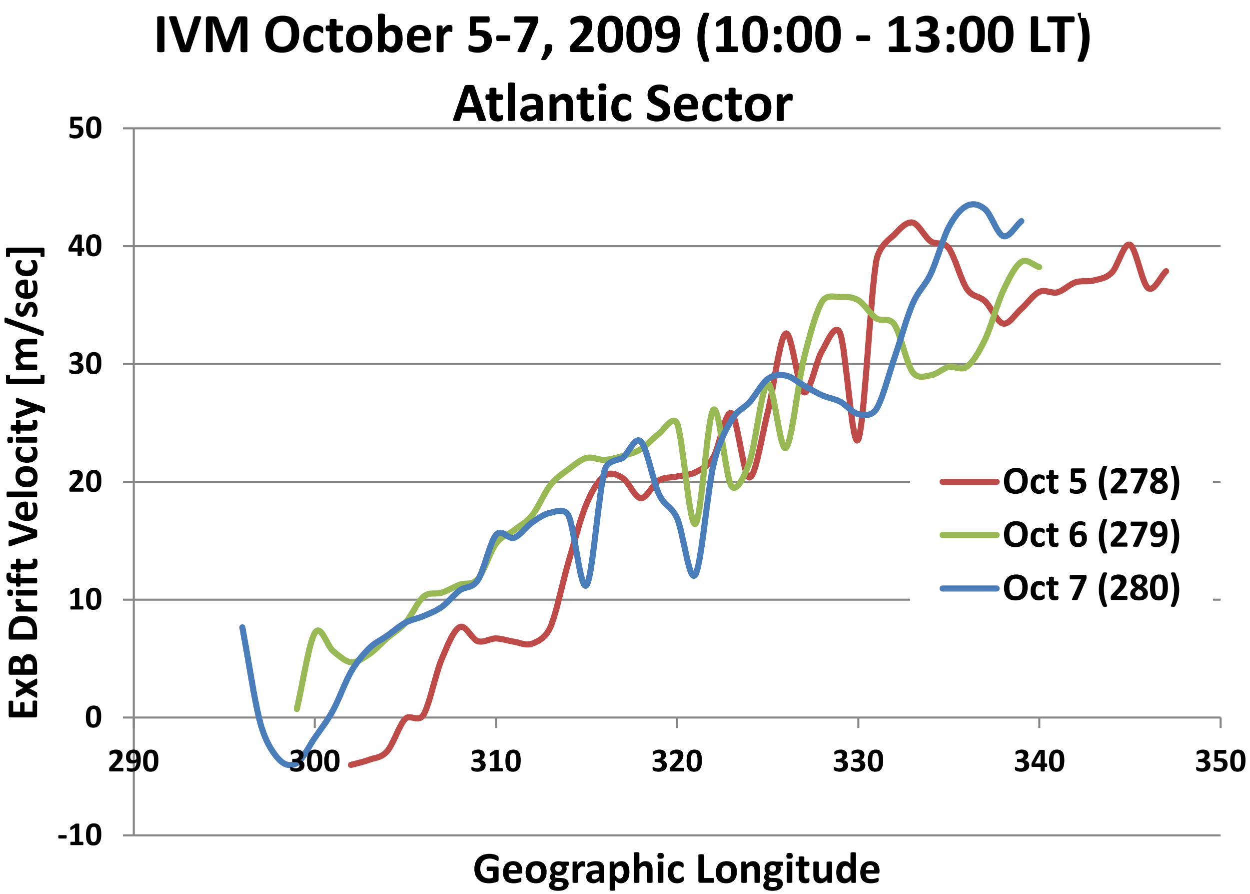

Longitude gradient in ExB drift ~ 1 m/sec/degree

Ground-based, Magnetometer-Inferred Daytime Vertical ExB Drift Velocities

EQUATORIAL ELECTROJET

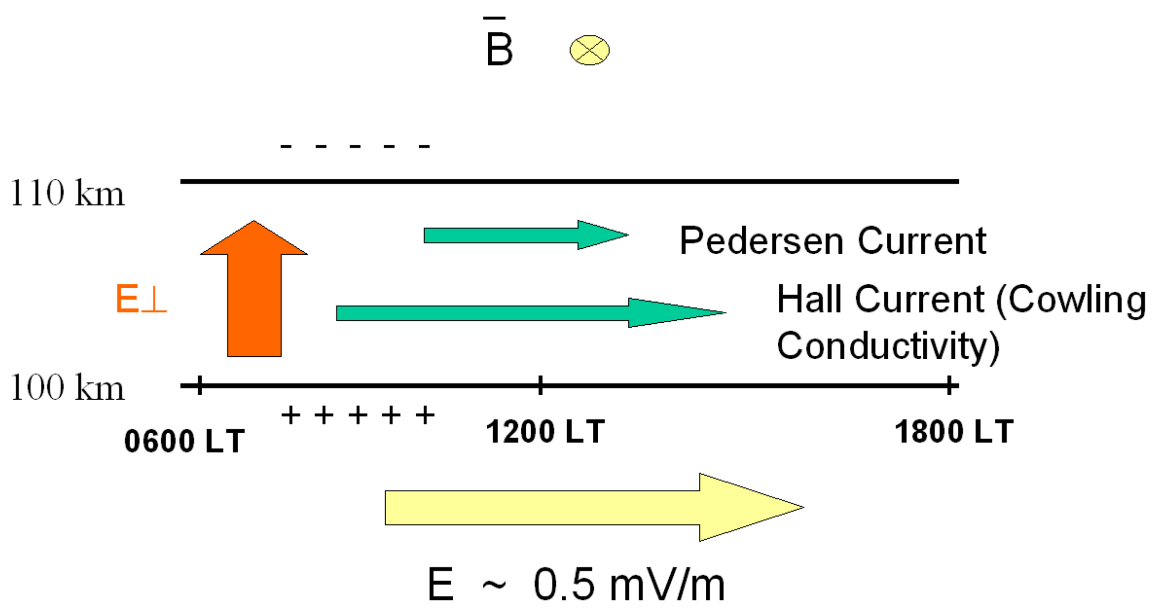

The contribution of the Equatorial Electrojet can be measured with 2 magnetometers. One at the Magnetic equator and another placed 6 or more away from magnetic equator.

Magnetic field

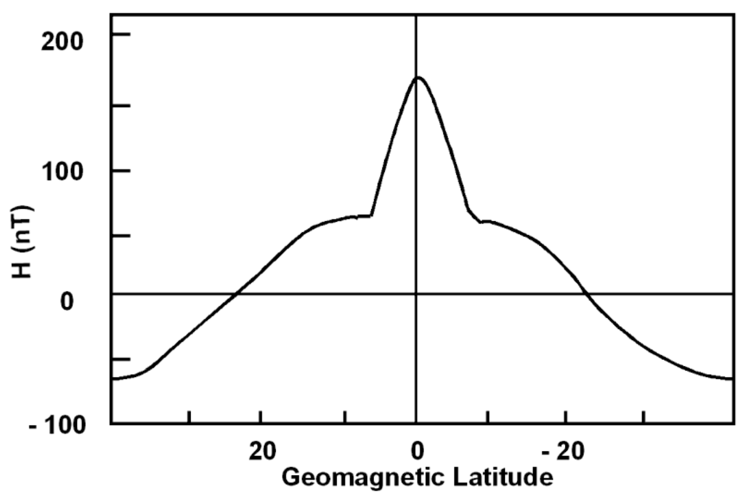

Comparing Magnetometer-inferred, Vertical ExB Drift Velocities Between Jicamarca and Alta Floresta Longitude Sectors for September 2 and 16

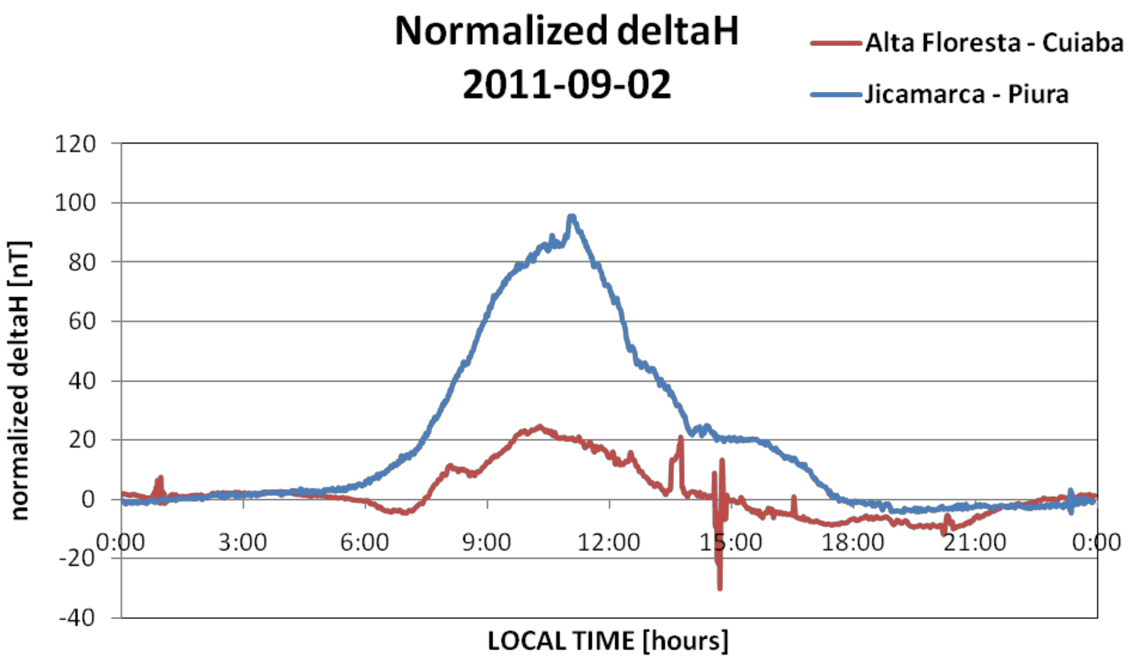

Assuming an ExB vs delta H linear slope of 0.31 m/sec/nT, the peak ExB drift velocity for Jicamarca-Piura is ~ 28 m/sec and for Alta Floresta-Cuiaba is ~6.5 m/sec.

On September 16, the peak ExB drift velocity is ~ 31 m/sec in the Jicamarca longitude sector and ~ 13 m/sec in the Alta Floresta longitude sector.

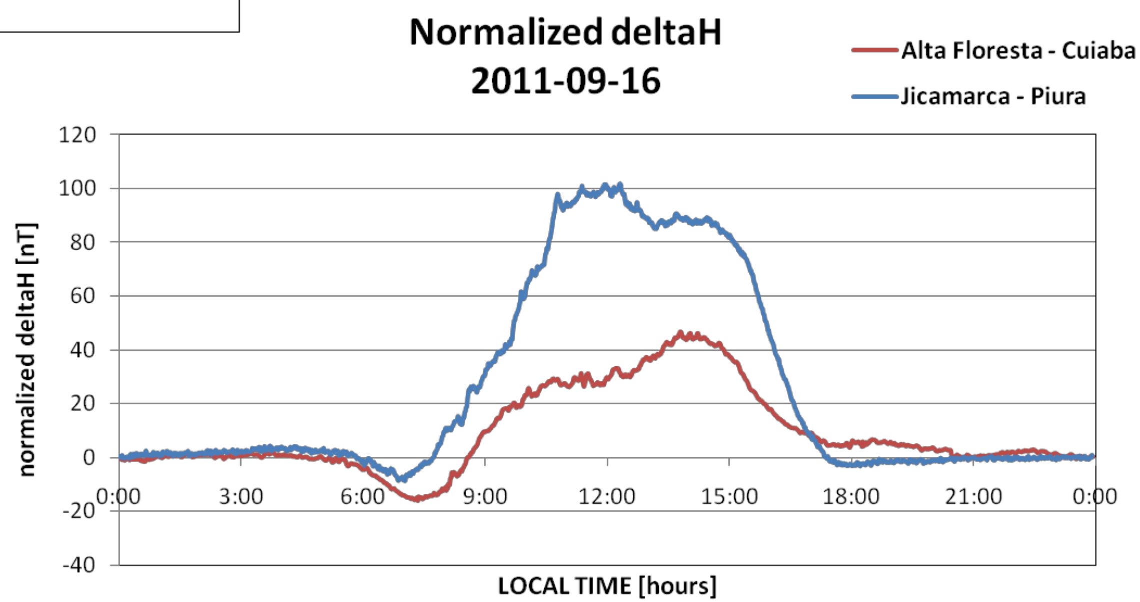

The combination of upward, daytime ExB drift velocity perpendicular to B and downward diffusion parallel to B by gravity and pressure gradient forces create crests in ionization at +/- 15 to 20 degrees magnetic latitude known as the equatorial anomaly. If the daytime, ExB drift velocities are significantly lower or are absent, then the crests in ionization are significantly closer to the magnetic equator or are absent

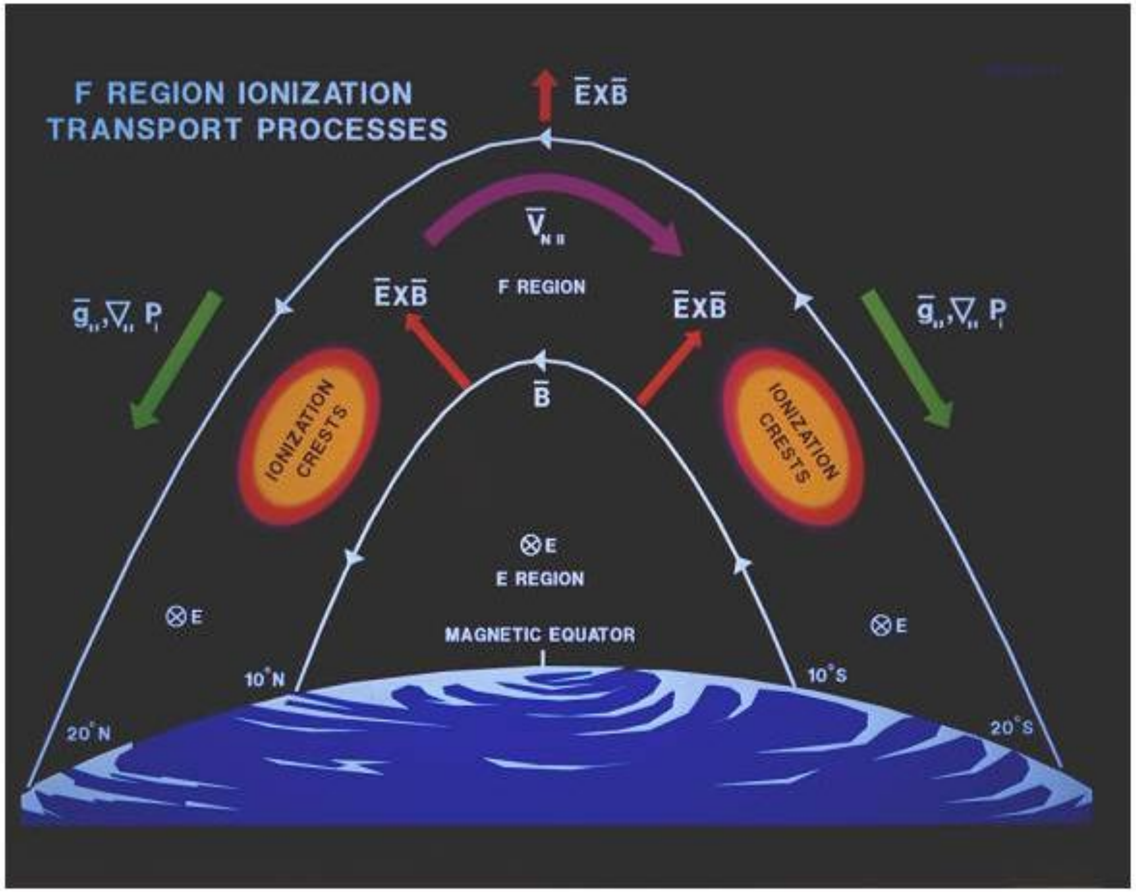

Provided by D. Anderson

Low Latitude Transport Mechanisms

TEC during the magnetic storm of August 3-4, 2010

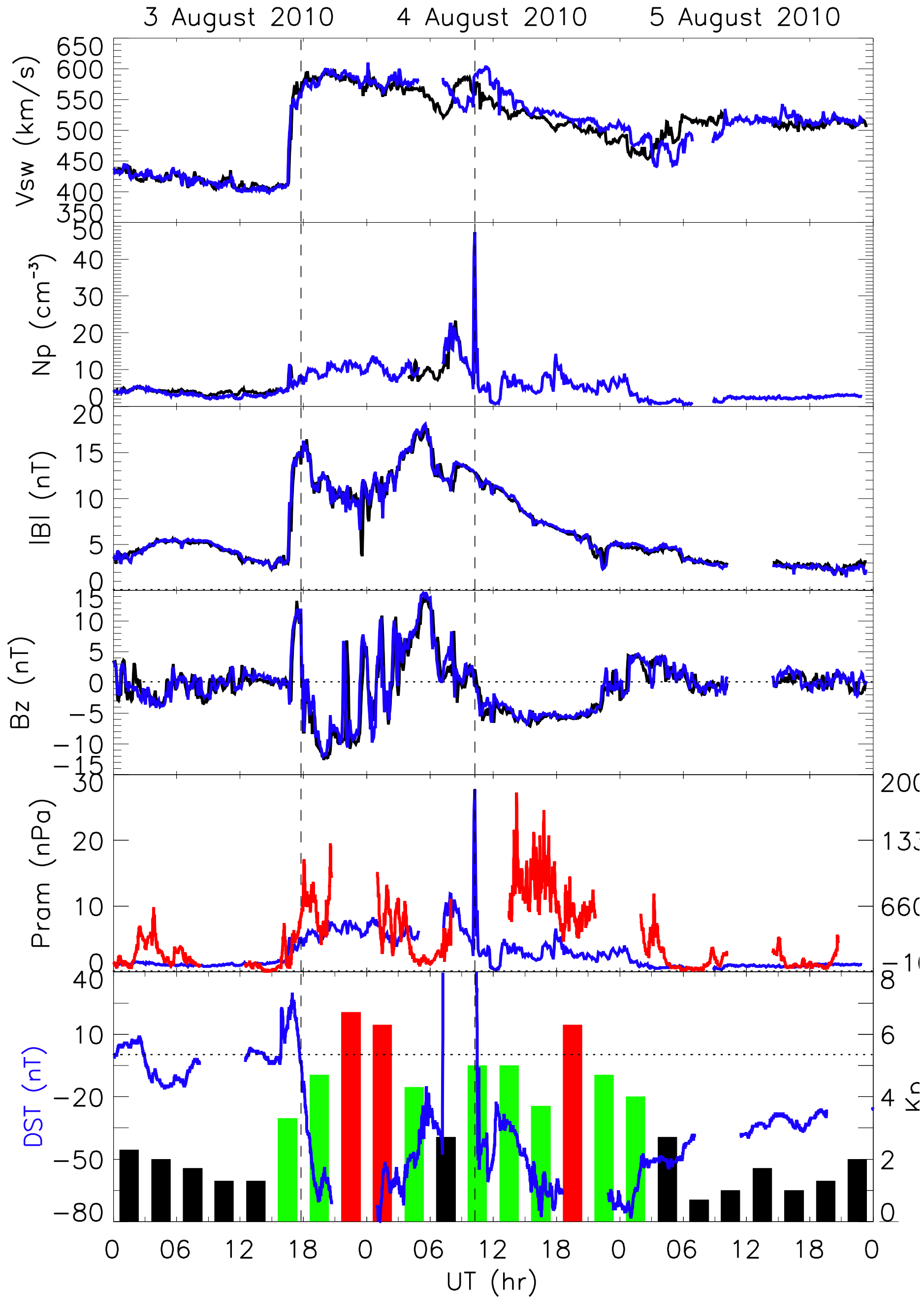

Provided by Endawoke

TEC values measured on August 03 - 04, 2010

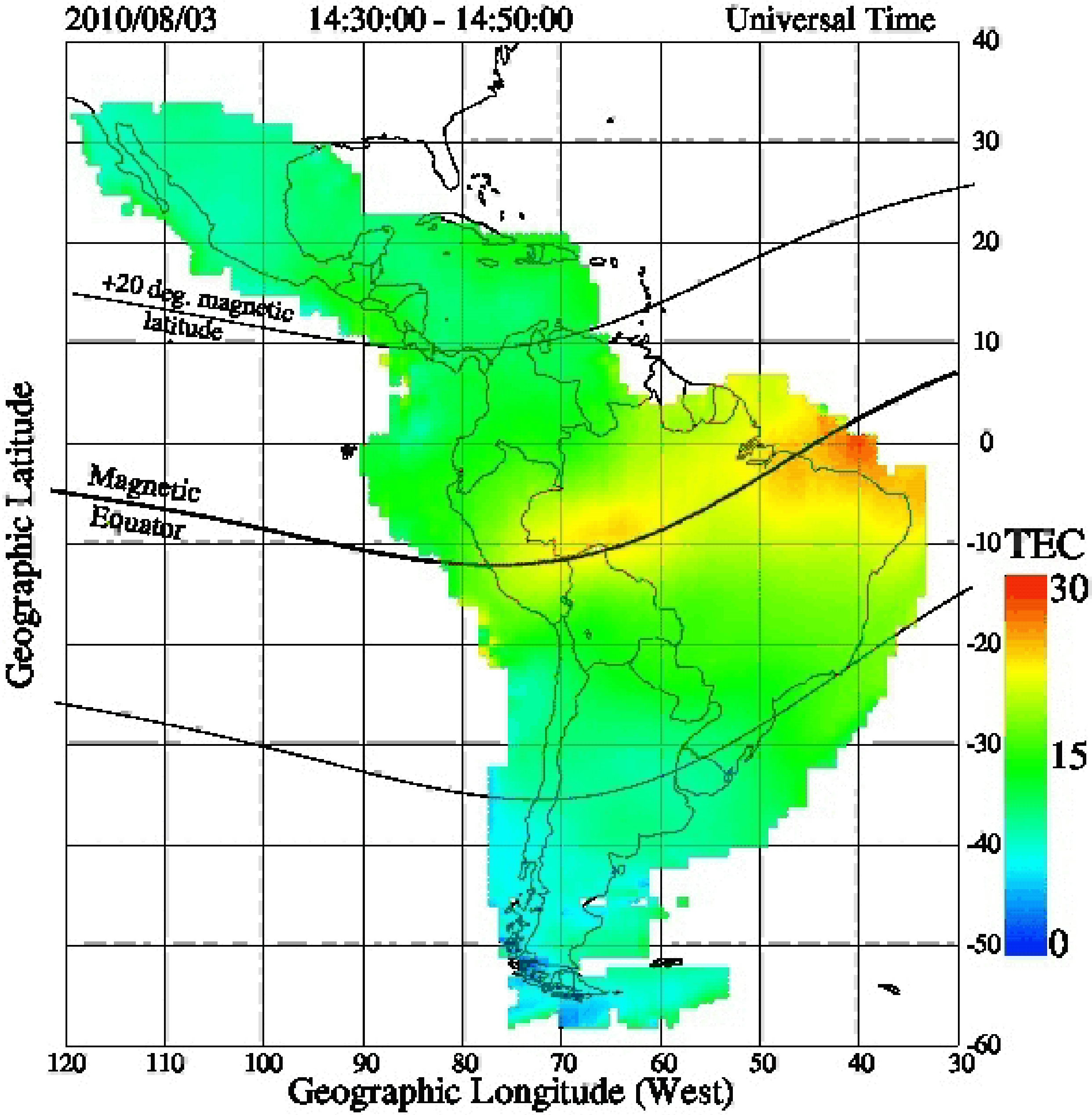

Longitudinal Extension of Anomaly during quiet magnetic conditions for August 01, 2010 (2 days before storm)

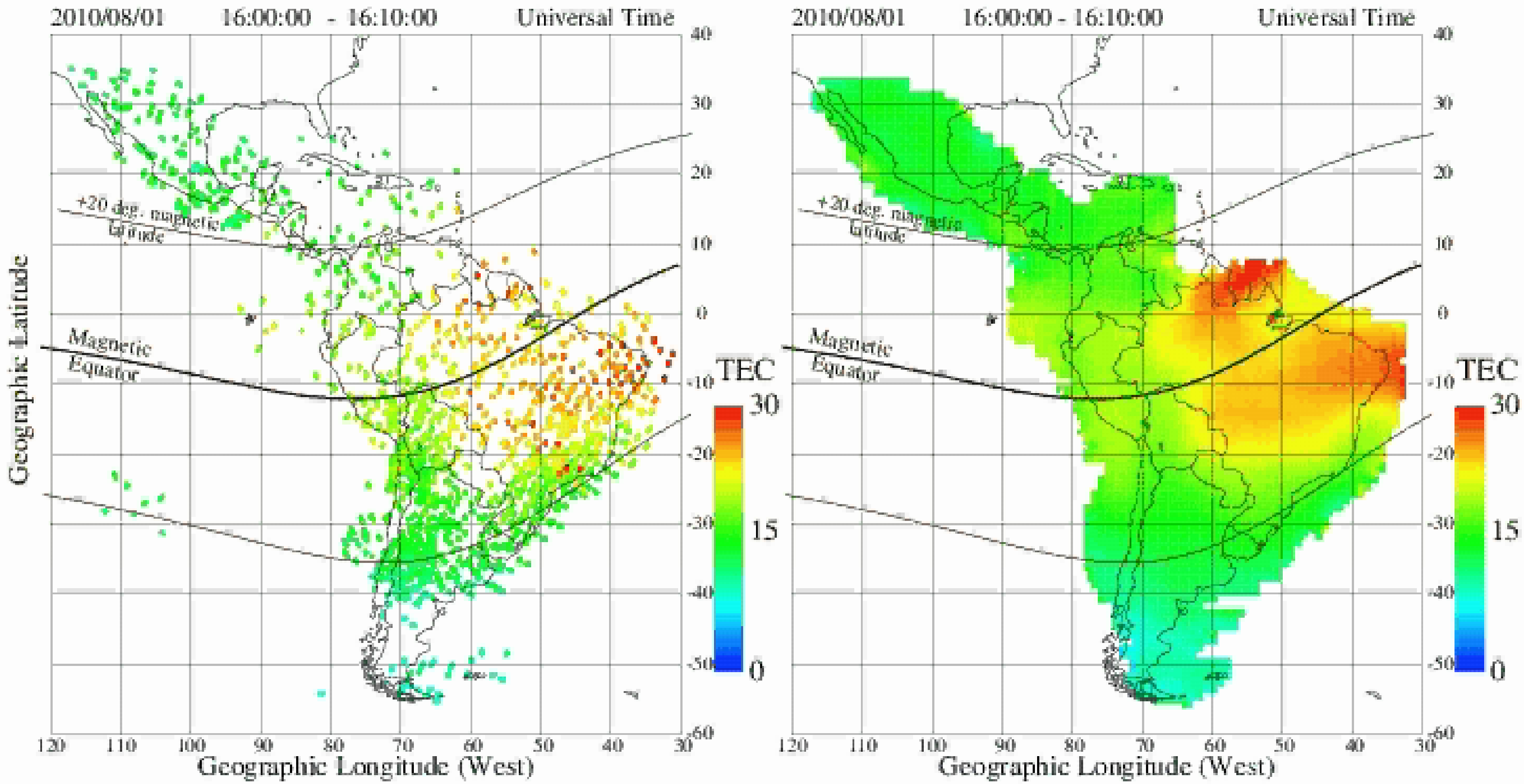

Longitudinal Extension of Anomaly during quiet magnetic cond.

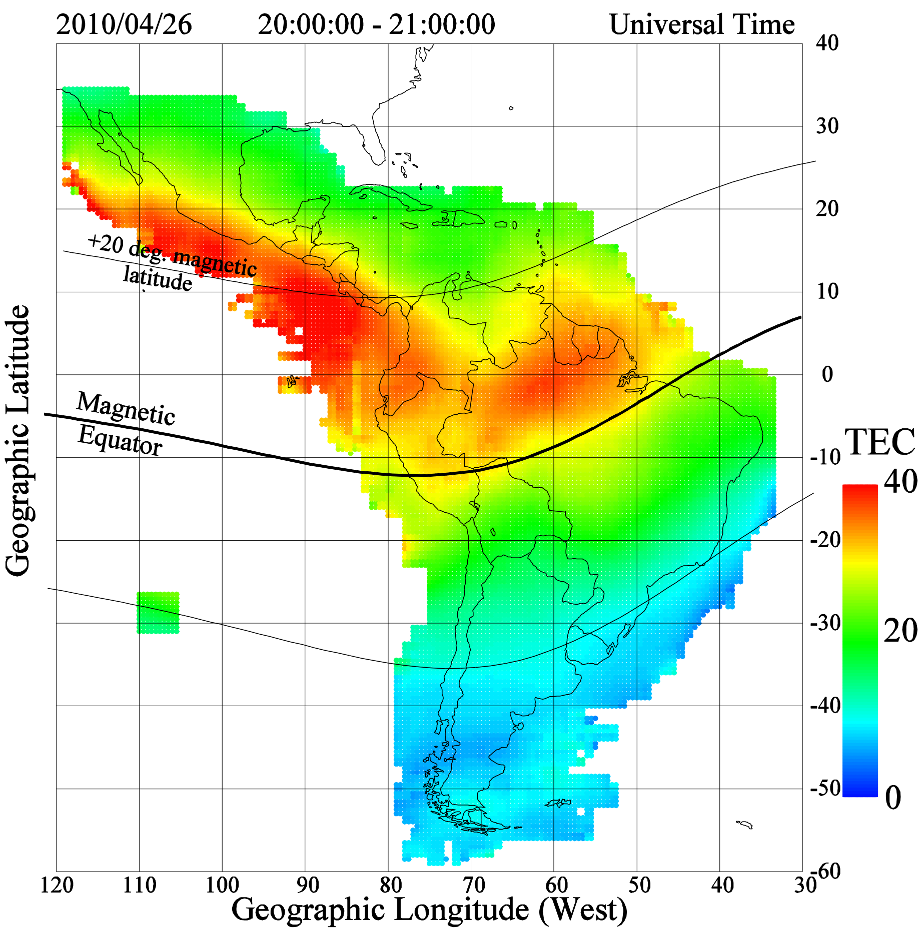

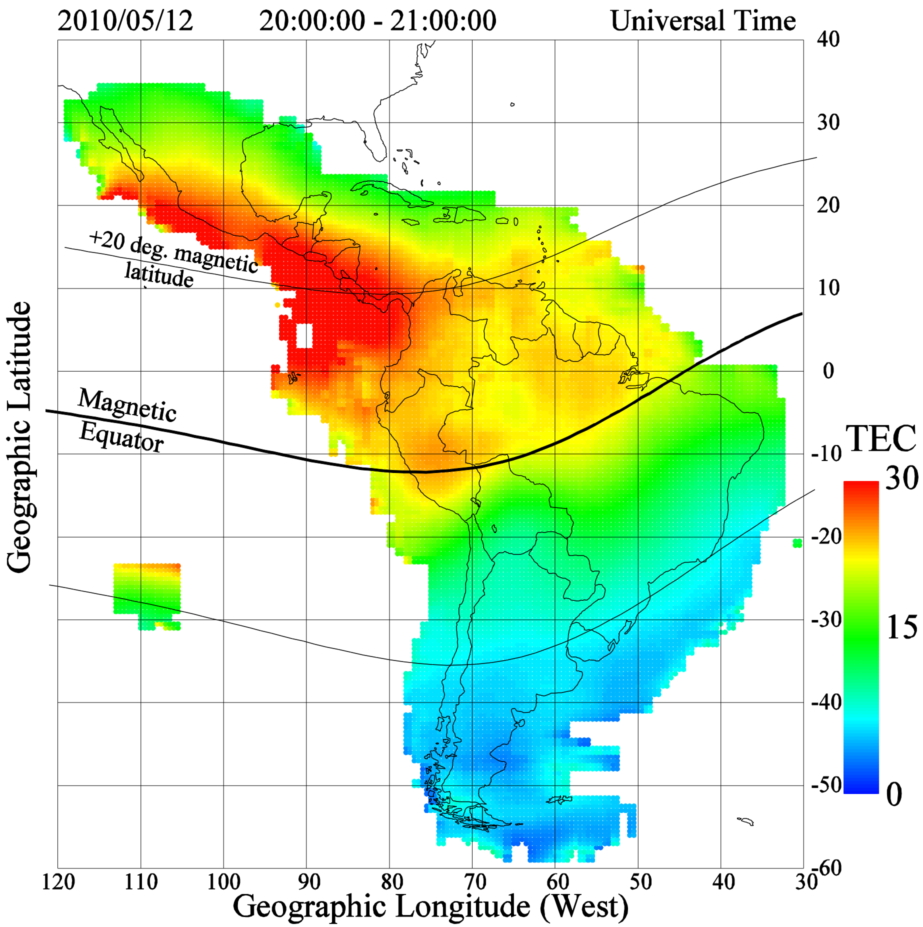

Longitudinal Extension of Anomaly during quiet magnetic cond.

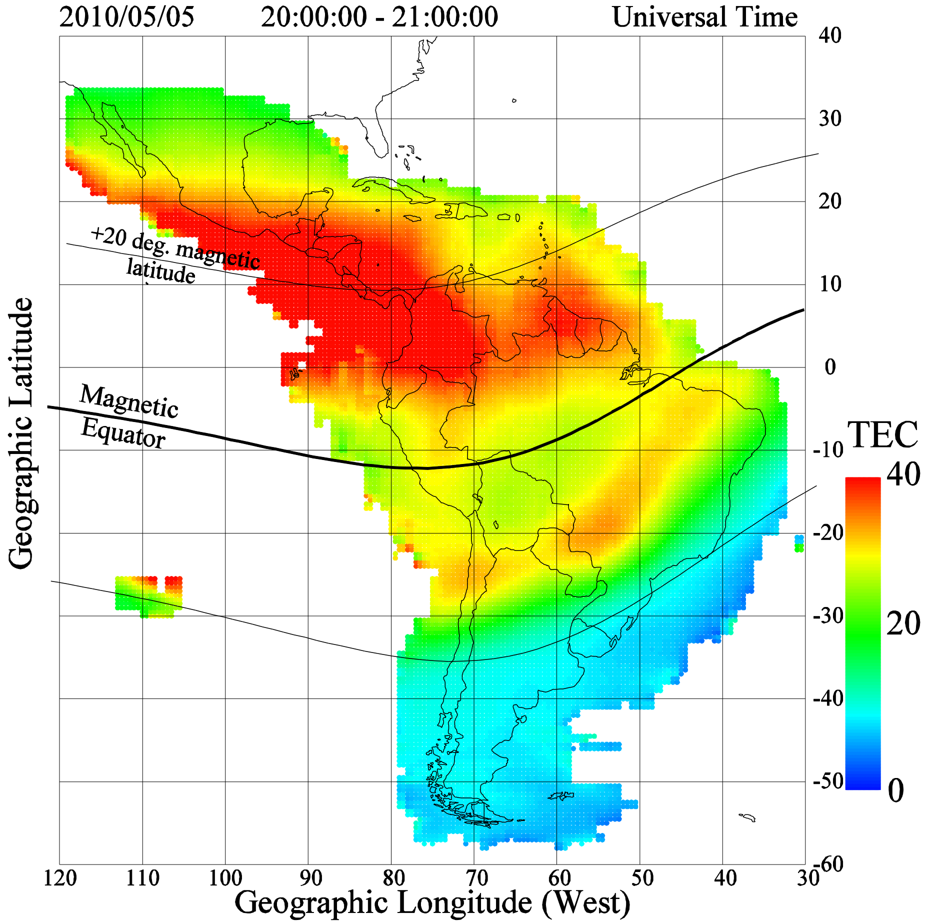

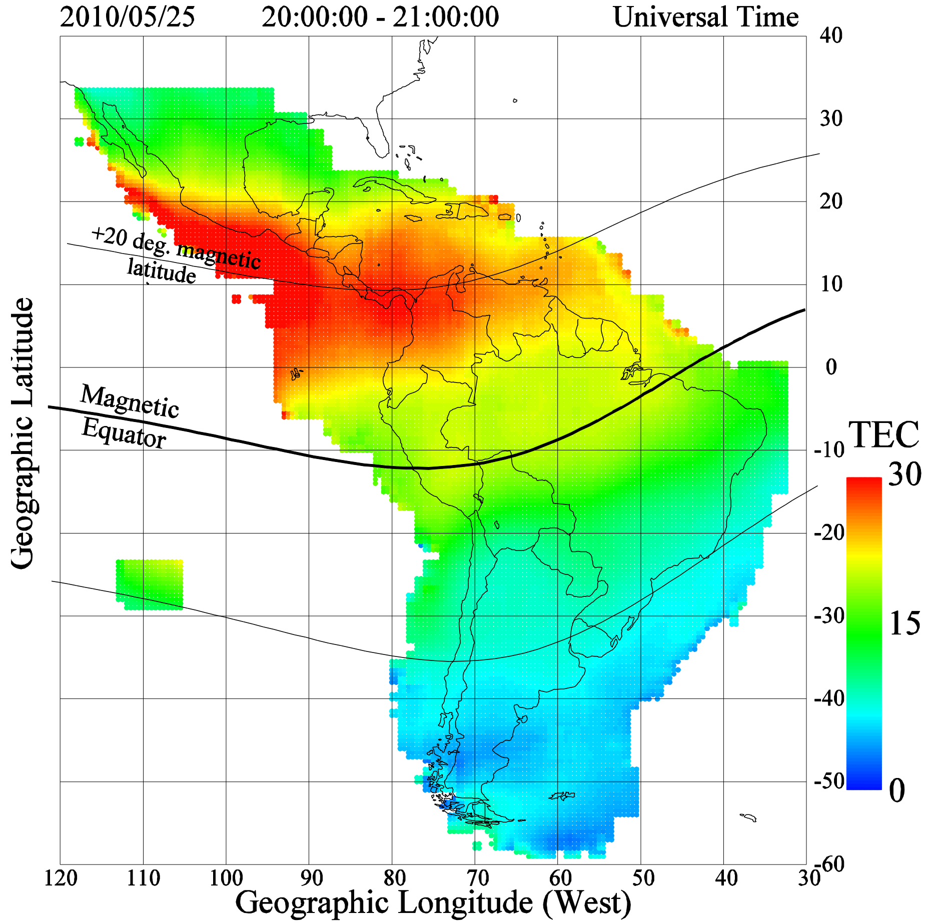

Conclusions

One of the main goals of the LISN network is to develop and forecasting capability of plasma bubbles (ESF) that examines the preconditioning of the low-latitude ionosphere in terms of TEC and density along the LISN meridian but also measures the seeding conditions in terms of the TIDs/GWs.

LISN will examine relationship between TIDs detected with GPSs and troposphere deep convection cells.


Molte Grazie
SECOND LOW-LATITUDE IONOSPHERIC SENSOR NETWORK WORKSHOP
São José dos Campos,SP Brazil - November 7-10, 2011
Sao Jose dos Campos, Nov 2011

TEC depletion Statistics

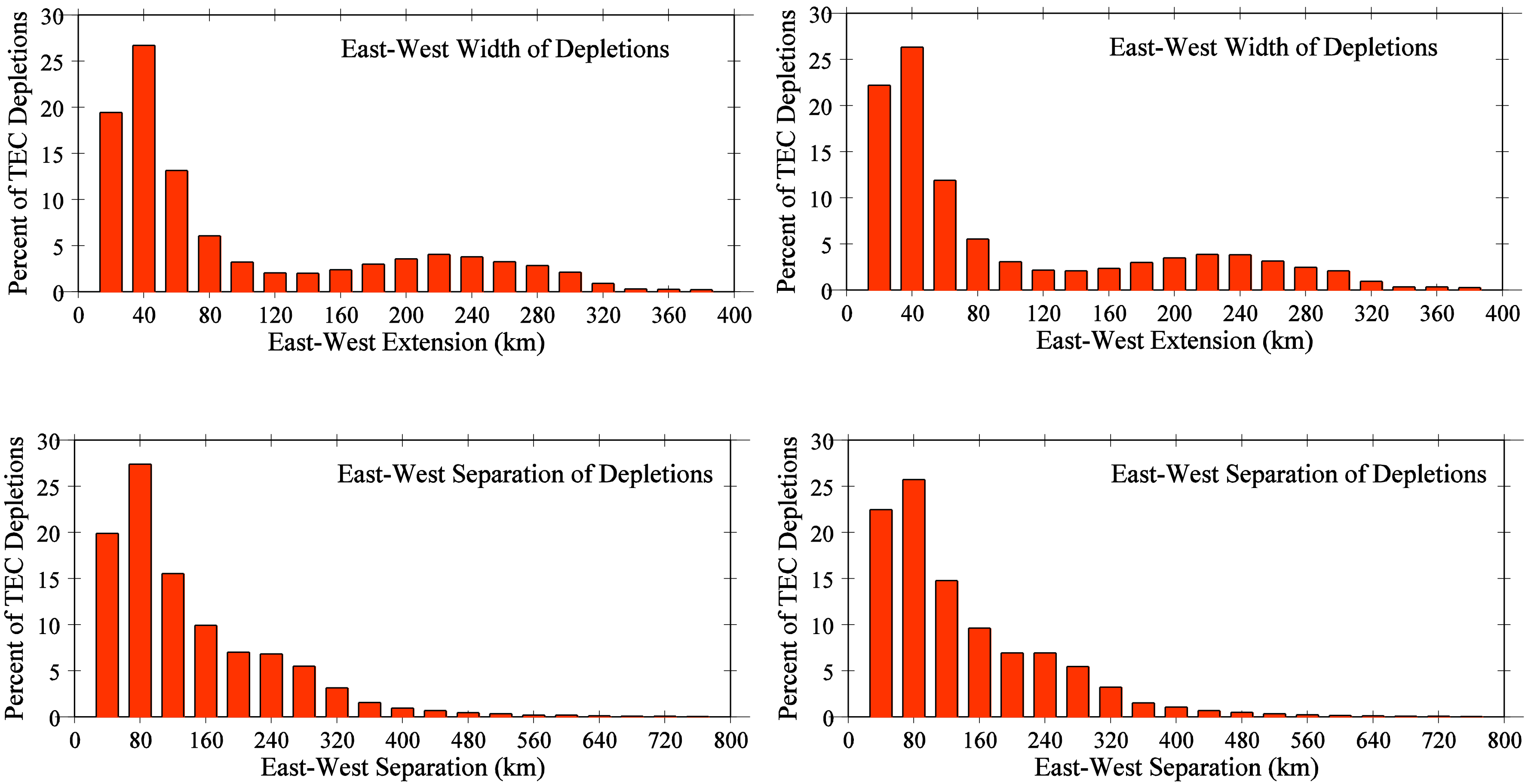

2009

2010

The Global Ionosphere Plasmasphere (GIP) theoretical, time-dependent ionospheric model has been used to calculate ion densities as a function of altitude, latitude, longitude and local time in the Peruvian and Atlantic longitude sectors to demonstrate the effects of sharp longitude gradients in ExB drift velocities on calculated ion density distributions

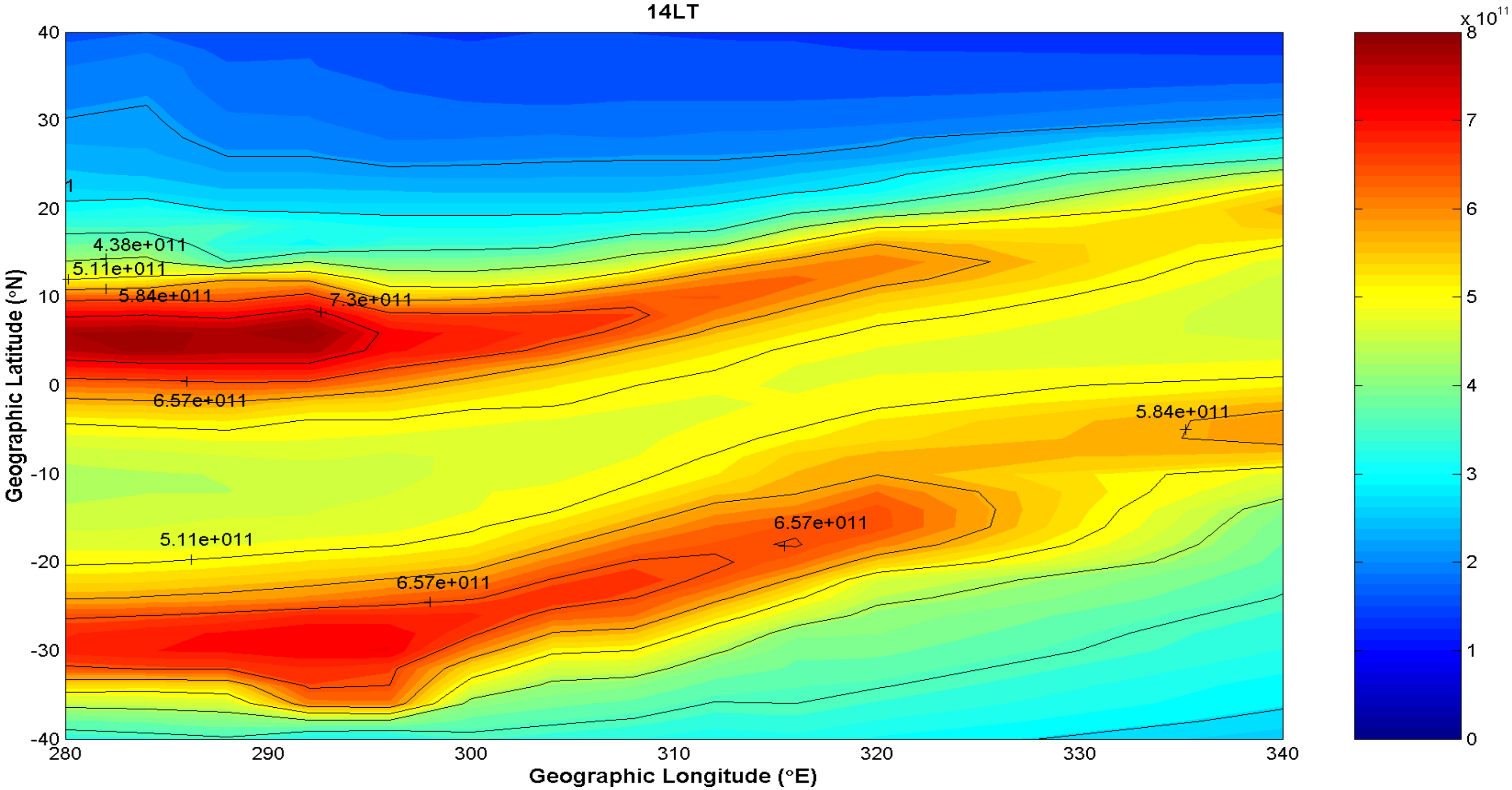

1st Ingredient of ESF Forecasting

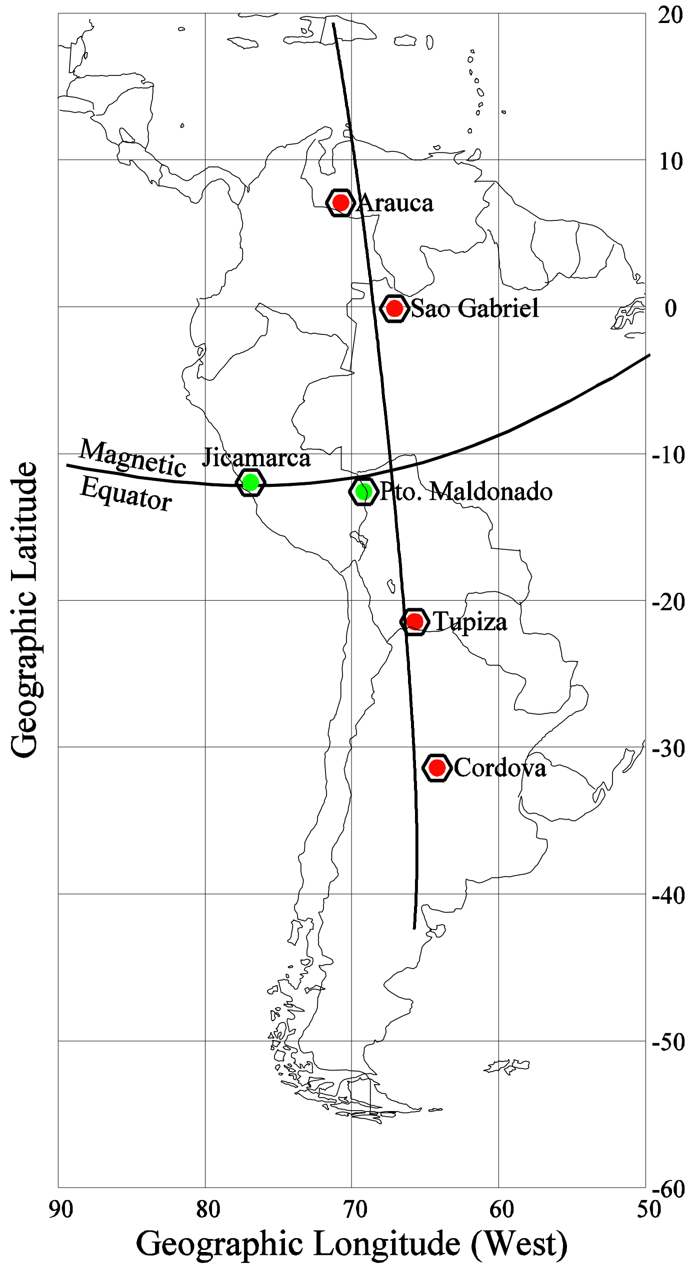

Bottomside density profiles from all 5 VIPIR ionosondes and GPS TEC data from 22 GPS receivers will be used in a tomographic reconstruction of density along the LISN meridian. The inversion technique will include regularization algorithms containing bottomside density profiles from the VIPIR ionosondes.

These latitudinal-heights densities can be used to calculate field line integrated conductivities and RTI Growth Rates.

Having density profiles as a function of latitude will help to get vertical drifts and meridional winds.

2nd Measurement of Seeding Conditions

Detection of TIDs/GWs in real time. Development of new algorithms to detect TEC small perturbation on real-time basis.

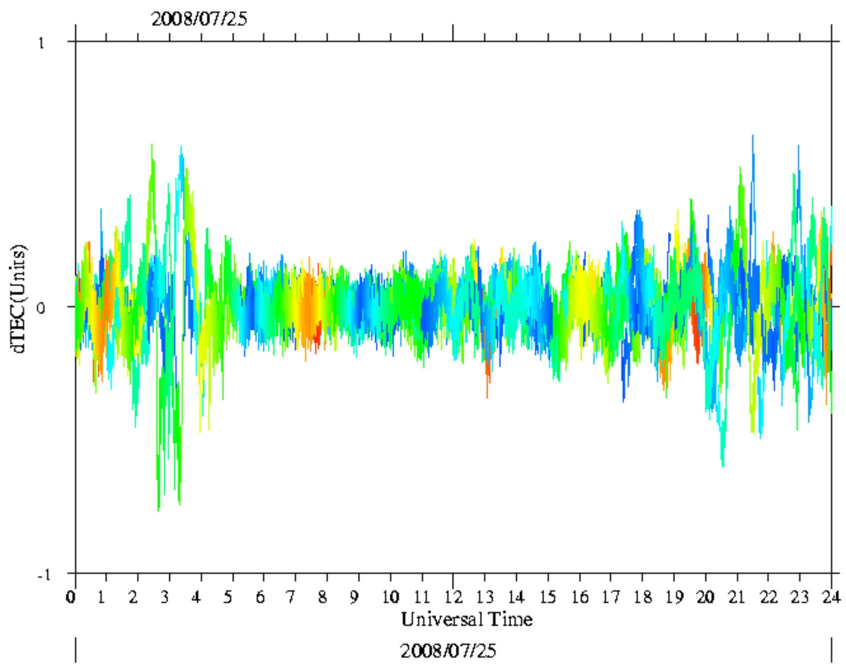

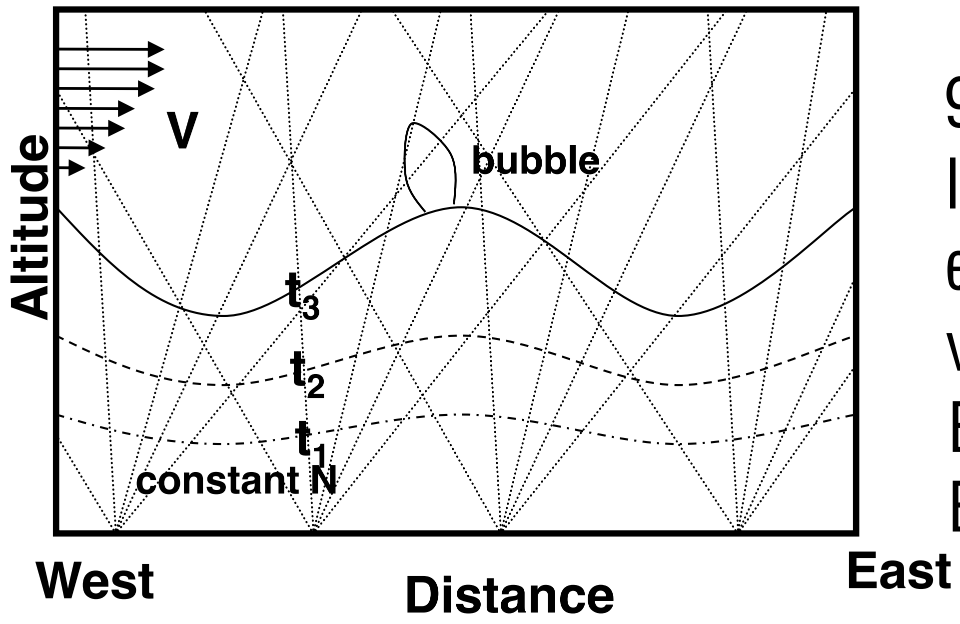

9 GPS receivers are presently located along the magnetic equator to observe the variability of TEC across Peru, Bolivia and the western part of Brazil.

Phase Velocity ($V_h(t)$) and Direction of Propagation ($\alpha(t)$) of TIDs using measured time delays between Huancayo , Iquitos and Cuzco.

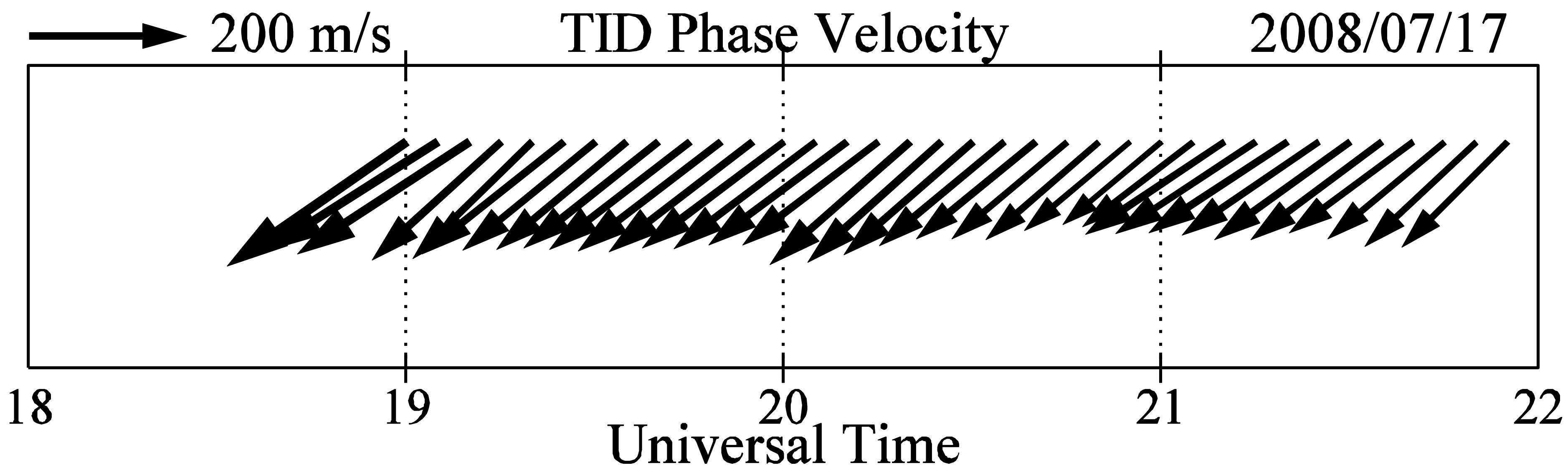

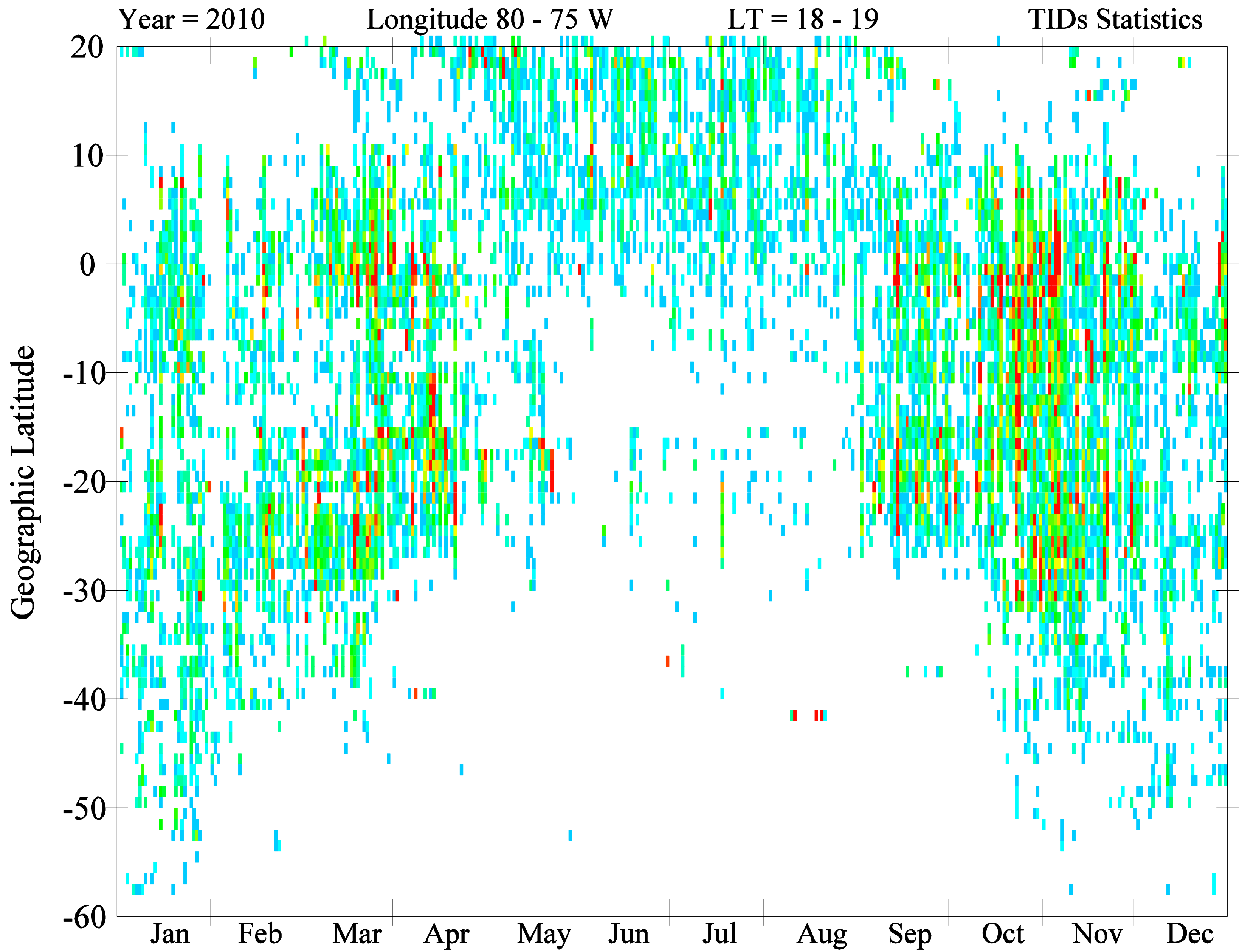
Year = 2010
Longitude 80 - 75 W
LT = 18 - 19
TIDs Statistics
Geographic Latitude
20
10
0
-10
-20
-30
-40
-50
-60
Jan
Feb
Mar
Apr
May
Jun
Jul
Aug
Sep
Oct
Nov
Dec

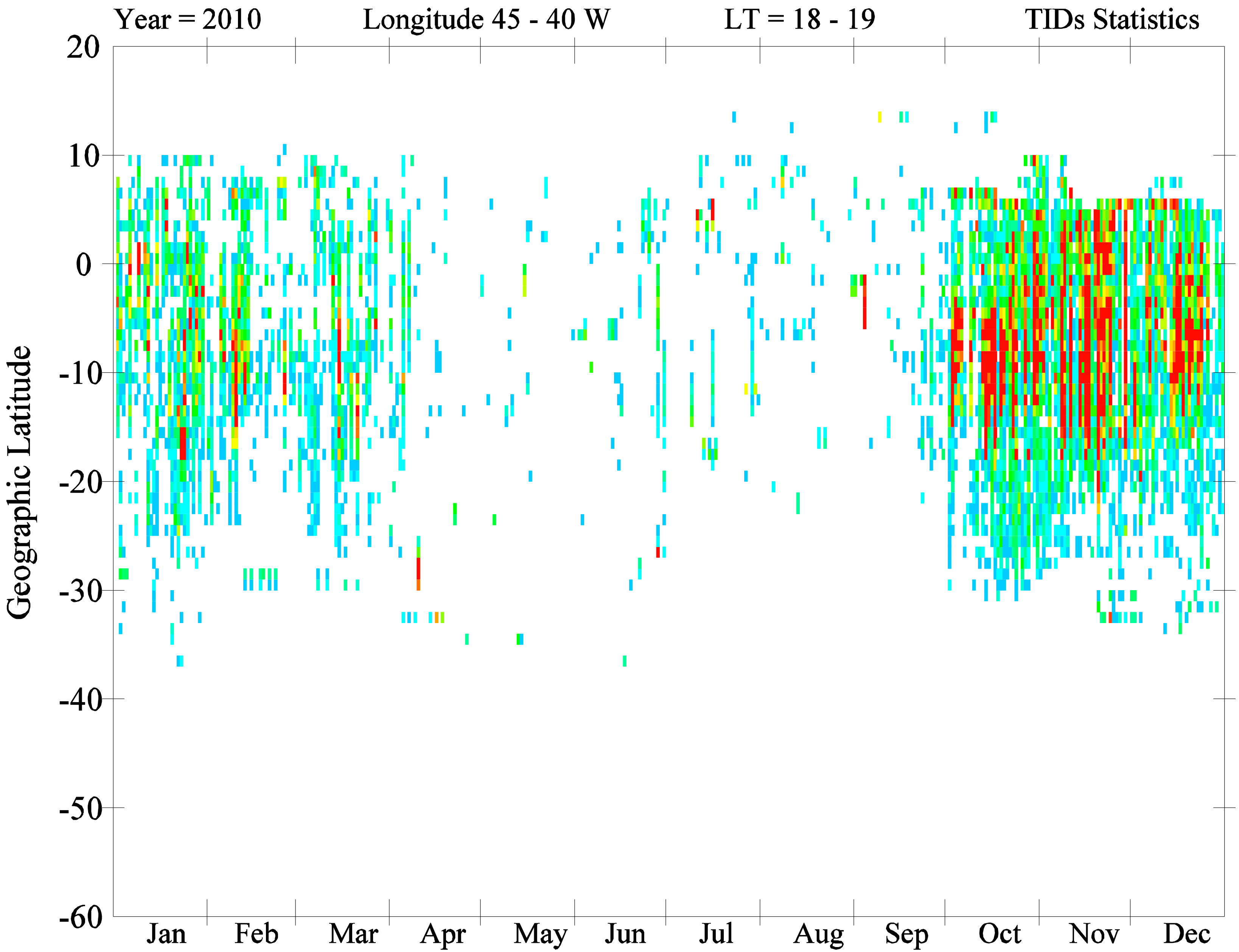
Year = 2010
Longitude 45 - 40 W
LT = 18 - 19
TIDs Statistics
Geographic Latitude
20
10
0
-10
-20
-30
-40
-50
-60
Jan
Feb
Mar
Apr
May
Jun
Jul
Aug
Sep
Oct
Nov
Dec

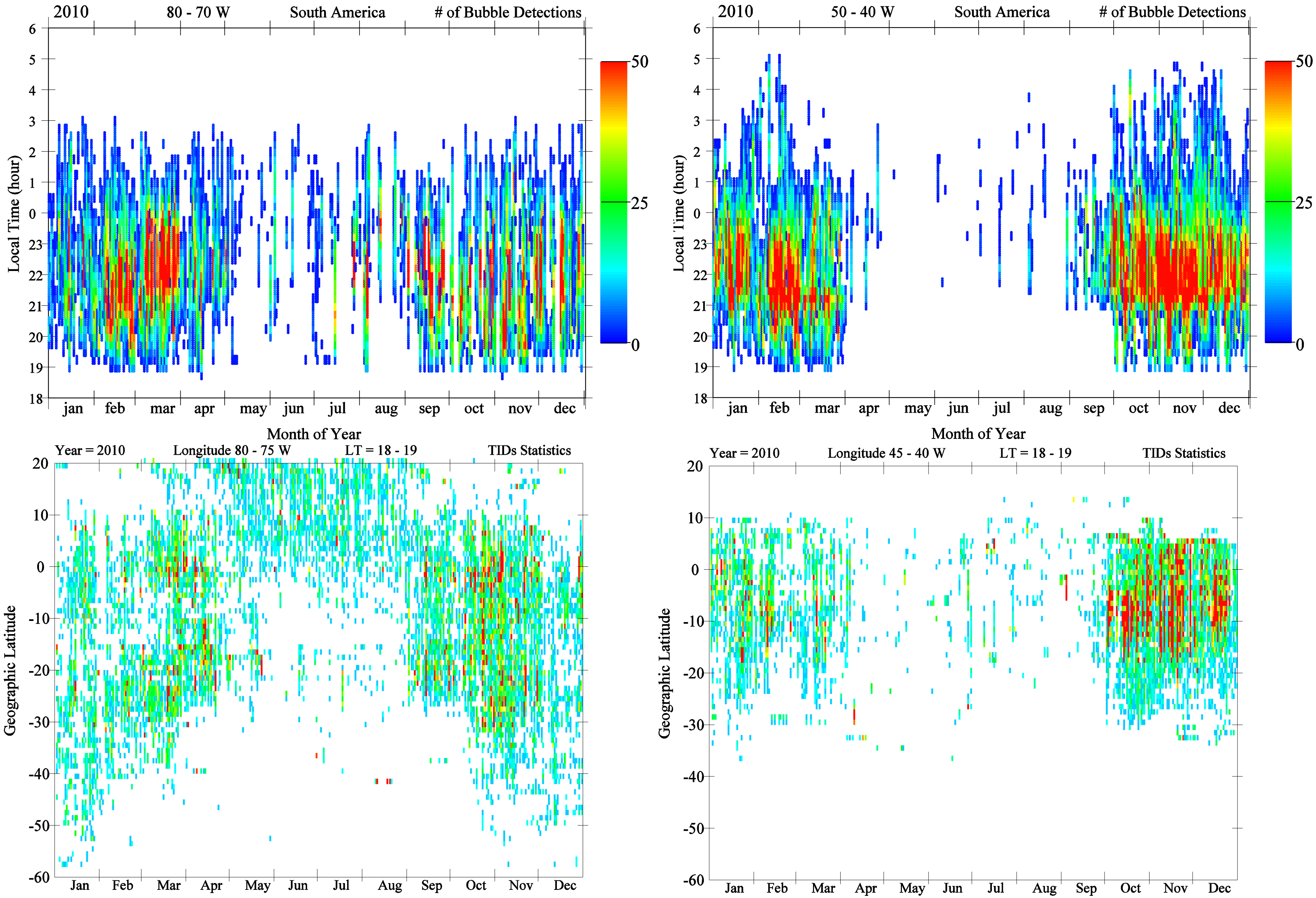
2010
80 - 70 W
South America
# of Bubble Detections
Local Time (hour)
Month of Year
jan feb mar apr may jun jul aug sep oct nov dec
2010
50 - 40 W
South America
# of Bubble Detections
Local Time (hour)
Month of Year
Year = 2010
Longitude 80 - 75 W
LT = 18 - 19
TIDs Statistics
Geographic Latitude
Jan Feb Mar Apr May Jun Jul Aug Sep Oct Nov Dec
Year = 2010
Longitude 45 - 40 W
LT = 18 - 19
TIDs Statistics
Geographic Latitude